AD-A040 115 DAVID W TAYLOR NAVAL SHIP RESEARCH AND DEVELOPMENT CE--ETC F/G 20/14
ANALYSIS OF THE OSCILLATORY MOTIONS OF THE MOORED BODY SCHEME A--ETC(U)
MAY 77 R CURPHEY

UNCLASSIFIED SPD-420-14 NL

1 OF 2
ADA040 115

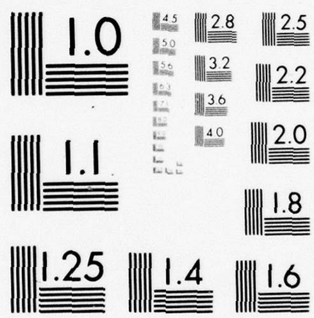
1.0
1.1
1.25
1.4
1.6
1.8
2.0
2.2
2.5
2.8
3.2
3.6
4.0
4.5
5.0
5.6

DAVID W. TAYLOR NAVAL SHIP
RESEARCH AND DEVELOPMENT CENTER
Bethesda, Md. 20084

ANALYSIS OF THE OSCILLATORY MOTIONS OF THE MOORED BODY SCHEME A IN WAVES AND CURRENT

by

R. Curphey

APPROVED FOR PUBLIC RELEASE: DISTRIBUTION UNLIMITED

Ship Performance Department

May 1977

SPD-420-14

ANALYSIS OF THE OSCILLATORY MOTIONS OF THE
MOORED BODY SCHEME A IN WAVES AND CURRENT

MAJOR DTNSRDC ORGANIZATIONAL COMPONENTS

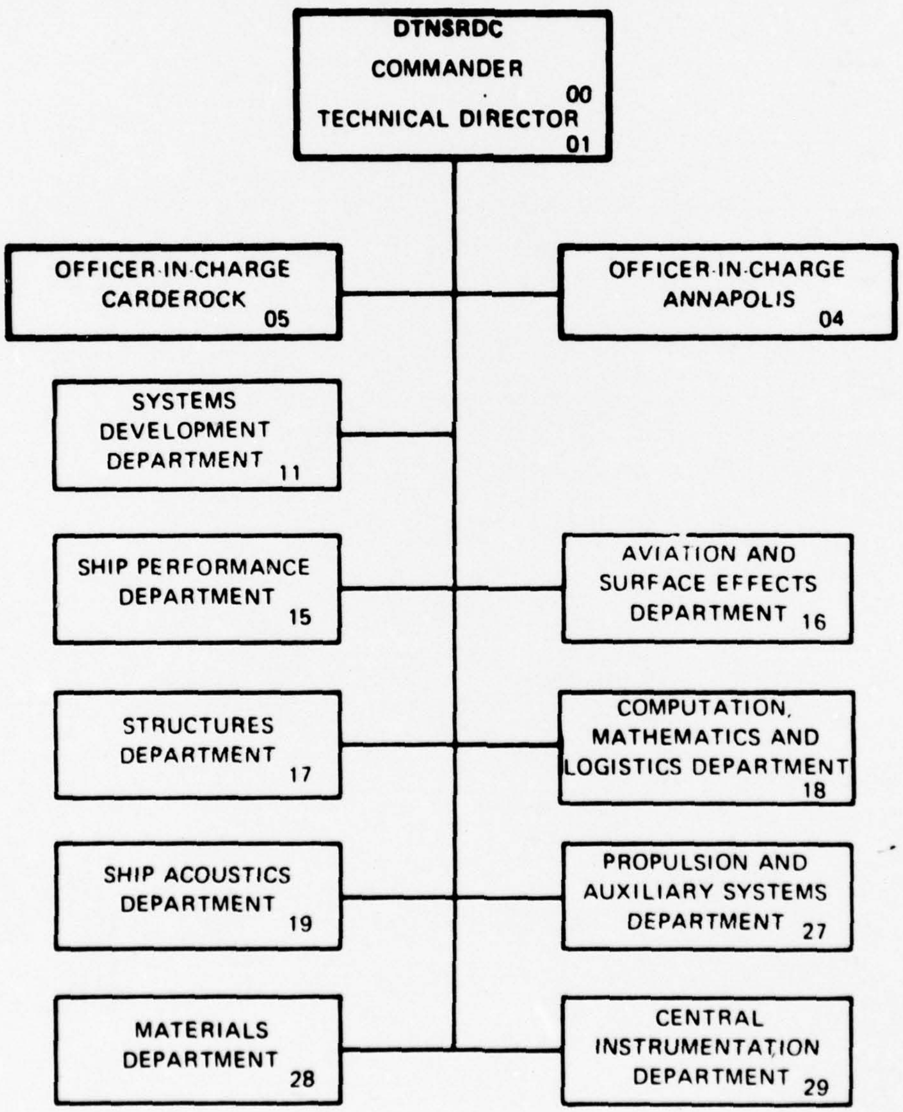

UNCLASSIFIED

SECURITY CLASSIFICATION OF THIS PAGE (When Data Entered)

REPORT DOCUMENTATION PAGE		READ INSTRUCTIONS BEFORE COMPLETING FORM
1. REPORT NUMBER 14 SPD-420-14	2. GOVT ACCESSION NO.	3. RECIPIENT'S CATALOG NUMBER
4. TITLE (and Subtitle) 6 Analysis of the Oscillatory Motions of the Moored Body Scheme A in Waves and Current.		5. TYPE OF REPORT & PERIOD COVERED 9 Final rept.,
		6. PERFORMING ORG. REPORT NUMBER
7. AUTHOR(s) 10 R. Curphey	UK	8. CONTRACT OR GRANT NUMBER(s)
9. PERFORMING ORGANIZATION NAME AND ADDRESS David W. Taylor Naval Ship R&D Center Bethesda, Maryland 20084		10. PROGRAM ELEMENT PROJECT, TASK AREA & WORK UNIT NUMBERS
11. CONTROLLING OFFICE NAME AND ADDRESS		12. REPORT DATE 11 May [redacted]77
		13. NUMBER OF PAGES 12 102p.
14. MONITORING AGENCY NAME & ADDRESS (if different from Controlling Office)		15. SECURITY CLASS (of this report) Unclassified
		15a. DECLASSIFICATION DOWNGRADING SCHEDULE

16. DISTRIBUTION STATEMENT (of this Report)

APPROVED FOR PUBLIC RELEASE: DISTRIBUTION UNLIMITED

17. DISTRIBUTION STATEMENT (of the abstract entered in Block 20, if different from Report)

18. SUPPLEMENTARY NOTES

19. KEY WORDS (Continue on reverse side if necessary and identify by block number)

Moored Body
Wave Forces and Moments
Current Forces and Moments
Potential Flow

20. ABSTRACT (Continue on reverse side if necessary and identify by block number)

This report describes a theoretical investigation of the oscillatory motions, stability, and orientation of the Moored Body Scheme A in current and waves. Linear, first order equations for oscillatory motions and cable tension, are developed for a body of revolution moored to the bottom in finite depth water by a single restraining cable. Wave exciting forces and certain hydrodynamic coefficients are developed from potential flow theory, and non-linear viscous damping effects are included in the formulation by an

over

DD FORM 1 JAN 73 1473 EDITION OF 1 NOV 65 IS OBSOLETE

S/N 0102-014-6601

UNCLASSIFIED

SECURITY CLASSIFICATION OF THIS PAGE (When Data Entered)

20. (Continued) equivalent linearization technique. Surge, sway, pitch, and yaw motion and tension amplitudes are obtained in response to regular and irregular waves for a variety of water depths, cable lengths, and static cable tensions. Equilibrium orientation in waves and currents is established by the current or wave-current interaction depending on the magnitude of body oscillation velocities relative to the current speed. The most prominent feature of the oscillatory motions is the presence of a pitch resonance occurring at a frequency of 0.33 radians per second.

TABLE OF CONTENTS

Page

ABSTRACT 1

INTRODUCTION 2

MOTION IN WAVES 4

EQUILIBRIUM CONDITIONS 4

EQUATIONS OF MOTION 9

Surge-Pitch 12

Sway-Yaw 13

Cable Tension 15

NONLINEAR DAMPING AND SOLUTION OF THE EQUATIONS 16

MOTION IN REGULAR WAVES 20

MOTION IN A SEAWAY 34

BODY ATTITUDE IN A STEADY CURRENT 48

STATIC EQUILIBRIUM 48

DYNAMIC STABILITY 54

Vertical Plane 55

Horizontal Plane 57

CABLE ORIENTATION 59

WAVE-CURRENT INTERACTIONS 61

CONCLUSIONS 64

ACKNOWLEDGMENTS 67

APPENDIX A - WAVE EXCITING FORCES 68

APPENDIX B - HYDRODYNAMIC COEFFICIENTS 76

APPENDIX C - EQUATIONS FOR DYNAMIC STABILITY 81

REFERENCES 88

LIST OF FIGURES

Page

Figure 1 - Sketch of the Moored Body Scheme A 5

Figure 2 - Definition Sketches of Moored Body Scheme A Geometry and Mooring System 7

Figure 3 - Effect of Non-linear Damping on Pitch Response in Regular Waves. 19

Figure 4 - Effect of Damping on the Peak Magnitude of the Pitch Response at Resonance in Regular Waves 19

Figure 5 - Effect of Wave Amplitude and Drag Coefficient on Pitch Angle at Resonance in Regular Waves. 19

Figure 6 - Effect of Water Depth on Surge Motion in Regular Waves. 24

Figure 7 - Effect of Water Depth on Pitch Motion in Regular Waves. 24

Figure 8 - Effect of Water Depth on Sway Motion in Regular Waves. 25

Figure 9 - Effect of Water Depth on Yaw Motion. 25

Figure 10 - Effect of Water Depth on Tension in Regular Waves 26

Figure 11 - Effect of Cable Length on Surge Motion in Regular Waves. 28

Figure 12 - Effect of Cable Length on Pitch Motion in Regular Waves 28

Figure 13 - Effect of Cable Length on Sway Motion in Regular Waves 29

Figure 14 - Effect of Cable Length on Yaw Motion in Regular Waves 29

Figure 15 - Effect of Cable Length on Tension in Regular Waves. . . . 30

Figure 16 - Effect of Static Cable Tension on Surge Motion in Regular Waves 31

Figure 17 - Effect of Static Cable Tension on Pitch Motion in Regular Waves 31

LIST OF FIGURES (Continued)

Page

Figure 18 - Effect of Static Cable Tension on Sway Motion in Regular Waves 32

Figure 19 - Effect of Static Cable Tension on Yaw Motion in Regular Waves 32

Figure 20 - Pierson-Moskowitz Sea Spectrum. 36

Figure 21 - Effect of Damping on Pitch Motion in Irregular Waves. . . 40

Figure 22 - Effect of Water Depth on Surge Motion in Irregular Waves. 41

Figure 23 - Effect of Water Depth on Pitch Motion in Irregular Waves. 41

Figure 24 - Effect of Water Depth on Yaw Motion in Irregular Waves. . 42

Figure 25 - Effect of Water Depth on Yaw Motion in Irregular Waves. . 42

Figure 26 - Effect of Water Depth on Tension in Irregular Waves . . . 43

Figure 27 - Effect of Cable Length on Surge Motion in Irregular Waves 44

Figure 28 - Effect of Cable Length on Pitch Motion in Irregular Waves 44

Figure 29 - Effect of Cable Length on Sway Motion in Irregular Waves 45

Figure 30 - Effect of Cable Length on Yaw Motion in Irregular Waves . 45

Figure 31 - Effect of Cable Length on Tension in Irregular Waves. . . 46

Figure 32 - Effect of Heading Angle on Motion and Tension in Irregular Waves 47

Figure 33 - Definition Sketch of Moored Body in a Steady Current. . . 49

Figure 34 - Static Pitch and Yaw Moment in a Steady Current 53

Figure 35 - Static Cable Deflection in a Steady Current 60

Figure 36 - Static Cable Tension in a Steady Current. 60

LIST OF TABLES

Page

Table 1 - Geometric Characteristics of the Moored Body Scheme A . . . 6

Table 2 - Resonant Frequencies of the Moored Body Scheme A. 22

Table 3 - The Pierson-Moskowitz Sea Spectrum. 37

Table 4 - Non-Dimensional Static Hydrodynamic Coefficients for Moored Body Scheme A. 51

Table 5 - Non-Dimensional Stability Derivatives for Moored Body Scheme A. 51

NOTATION

Symbol	Definition
$a_{22}(x)$, $a_{33}(x)$	Sectional added mass in sway and heave modes, respectively
A	Incident wave amplitude
$A_{1/3}$	Significant amplitude
A_{ij}	Added inertia coefficients (i, j = 1, surge; 2, sway; 3, heave; 5, pitch; 6, sway)
B	Buoyancy
B_{ij}	Damping coefficients (i, j = 1, 2, 3, 5, 6; see definition of A_{ij})
C_D	Drag coefficient for circular cylinder
$D(x)$	Diameter of body at longitudinal location x
$\vec{F}$	Total wave exciting force acting on body
F_D	Generalized viscous drag force
F_i	Component of wave exciting force and moment (i = 1, longitudinal force, 2, lateral force; 3, vertical force; 5, pitch moment; 6 yaw moment)
F_{oi}	Complex amplitude of F_i (i = 1, 2, 3, 5, 6)
g	Acceleration due to gravity
G_{ij}	Constants for viscous drag
h	Water depth
h_B	Distance from bottom to baseline of body
h_c	Distance from bottom to longitudinal axis of body
$h_{1/3}$	Significant waveheight
i	Denotes $\sqrt{-1}$ (when not used as a subscript)
I_y, I_z	Moment of inertia about y and z axes, respectively

NOTATION (Continued)

Symbol	Definition
K	Wave number of incident wave $(2\pi/\lambda)$
L	Length of body
m	Mass of body
M	Pitch moment on body in a current about center of gravity
M_T	Pitch moment on body in a current about y' axis
$\vec{M}$	Total wave exciting moment acting on body relative to the Oxyz system
$\vec{n}$	Unit normal surface vector (positive into body)
n_1, n_2, n_3	Components of $\vec{n}$ in x, y, z directions, respectively
n_4, n_5, n_6	Components of $(\vec{r}_o \times \vec{n})$ in the x, y, z directions, respectively
N	Yaw moment on body in a current about center of gravity
N_T	Yaw moment on body in a current about z' axis
Oxyz	Right-handed, inertial, Cartesian coordinate system located at equilibrium body position with origin on longitudinal axis above cable attachment point (See Figure 2)
Ox'y'z'	Right-handed, body fixed, Cartesian coordinate system with origin on longitudinal axis above cable attachment point (See Figure 33)
p	Hydrodynamic pressure
q, r	Perturbation angular velocity about y' and z' axes, respectively, for body in a current
r', θ, x'	Body fixed cylindrical coordinate system with origin at Oxyz.
$\vec{r}_o$	Vector from origin of Oxyz to a point on the body surface
R(x)	Radius of body at longitudinal location x

NOTATION (Continued)

Symbol	Definition
R_o	Maximum body radius
$R_S(\omega)$	Response amplitude operator
s	Laplace operator, $\frac{d}{dt}$
$S(\omega)$	Sea spectrum
S_o	Denotes body surface
$S_A(x)$	Cross sectional area at location x
T	Total cable tension
T_s	Static cable tension
T_{snap}	Tension required to break cable
T_3	Oscillatory component of cable tension
T_{o_3}	Complex amplitude of T_3
t	Time
$v_i(x)$	Generalized velocity of body at location x
u, v, w	Perturbation velocities in x', y', z' directions, respectively, for body in a current
u_o, v_o, w_o	Negative components of current speed in x', y', z' directions, respectively, for body in a current
U_o	Current speed
W	Weight
x, y, z	Right-handed, inertial, Cartesian coordinates (See definition of Oxyz and Figure 2)
x', y', z'	Right-handed, body fixed, Cartesian coordinates (See definition of Ox'y'z' and Figure 33)
x_B, x_G	Longitudinal coordinate of centers of buoyancy and gravity, respectively, relative to the Oxyz system

NOTATION (Continued)

Symbol	Definition
Y, Z	Lateral and vertical force acting on body in a current
z_B, z_G	Vertical coordinate of centers of buoyancy and gravity, respectively, relative to the Oxyz system
α_o	Equilibrium angle in vertical plane which body makes with the steady current
β	Wave heading angle relative to body x axis
β_o	Equilibrium angle in horizontal plane which body makes with the steady current
γ	See Equation (A6)
δ	See Equation (A6)
θ	Angular coordinate about body longitudinal axis
θ_D	Static cable deflection angle from vertical
λ	Wavelength
ξ_i, $\dot{\xi}_i$, $\ddot{\xi}_i$	Components of body displacement, velocity, and acceleration, respectively, in waves (i = 1, surge; 2, sway; 3, heave; 5, pitch; 6, yaw)
ξ_{oi}	Complex amplitude of ξ_i (i = 1, 2, 3, 5, 6; See definition of ξ_i)
ρ	Mass density of water
σ'	Nondimensional stability root
φ_2, φ_3	Two-dimensional forced oscillation potentials for sway and heave motion, respectively
Φ	Total velocity potential
Φ_D	Velocity potential of diffracted wave
Φ_I	Velocity potential of incident wave
Ψ_i	Perturbation displacements relative to the body fixed system Ox'y'z' (i = 1, surge; 2, sway; 3, heave; 5, pitch; 6, yaw)
ω	Wave angular frequency

UNITS

Most of the values given in the text and figures are in U.S. Customary Units. The equivalent values in the International System (SI) can be determined as follows:

1 foot	0.3048 metre
1 pound	4.448 newton
1 slug	14.59 kilogram
1 knot	0.5144 metre/second
1 $foot^2$	0.09290 $metre^2$
1 $foot^3$	0.02831 $metre^3$
1 pound/foot	14.59 newton/metre
1 foot-pound	1.356 newton-metre

ABSTRACT

This report describes a theoretical investigation of the oscillatory motions, stability, and orientation of the Moored Body Scheme A in current and waves. Linear, first-order equations for oscillatory motions and cable tension are developed for a body of revolution moored to the bottom in finite depth water by a single restraining cable. Wave exciting forces and certain hydrodynamic coefficients are developed from potential flow theory, and non-linear viscous damping effects are included in the formulation by an equivalent linearization technique. Surge, sway, pitch, and yaw motion and tension amplitudes are obtained in response to regular and irregular waves for a variety of water depths, cable lengths, and static cable tensions. Equilibrium orientation in waves and currents is established by the current or wave-current interaction depending on the magnitude of body oscillation velocities relative to the current speed. The most prominent feature of the oscillatory motion is the presence of a pitch resonance occurring at a frequency of 0.33 radians per second.

INTRODUCTION

The David W. Taylor Naval Ship R&D Center (DTNSRDC) was requested to analytically determine the oscillatory motions and orientation of a moored body under a seaway and subject to a current. Moored Body Scheme A, which is assumed to have a circular cross-section, is statically tethered at a prescribed height above and parallel to a smooth horizontal bottom by a single cable attached to a point on the body forward of the center of gravity. The body may be subject to the forces and moments induced by a train of regular, surface waves propagating through the finite depth water at an arbitrary angle relative to the body, the forces and moments resulting from a small steady current, or the combination of both waves and current.

It is required that the oscillatory surge, sway, pitch and yaw motions, and the variation in the cable tension (roll is not considered) be determined over a range of sea states as a function of water depth, cable length, static cable tension, and wave heading angles. It is further required that the body orientation and cable deflection angle in a steady current and any possible interaction between a small current and waves be determined.

The first section of this report describes the theoretical formulation and presents motion results for the moored body subject to incident waves with no current present. The formulation of the equations of motion and tension fluctuations is linear and harmonic with respect to wave amplitude and body motions. Heave motion is assumed to be restrained by the cable. The equations are coupled in the surge and pitch modes and the sway and yaw modes and contain appropriate linear cable tension functions. The

wave exciting forces and moments and the added inertia coefficients which include the effect of the bottom and finite depth water are developed from potential theory. Viscous damping effects, which are nonlinear in nature, are also incorporated in the equations by an equivalent linearization technique.

Amplitudes of the surge, sway, pitch, and yaw motion, and the cable tension fluctuations in response to incident sinusoidal waves of unit amplitude are presented as a function of excitation wavelength for various water depths, cable lengths, static cable tensions, and heading angle conditions. In addition, the regular wave responses have been used to obtain the statistical motion and tension in an irregular sea defined by the Pierson-Moskowitz Sea Spectrum.

In the second section of the report, the orientation of the body in a steady current is investigated. The static and dynamic stability of the Moored Body Scheme A in the pitch and yaw planes is determined based upon hydrodynamic coefficients obtained from model tests on a configuration similar to Scheme A. Once the stable pitch and heading angle relative to the current are known, the static cable tension and deflection angle are determined.

In the last section the interaction of current and waves is briefly examined. For current speeds which are less than or of the same order as oscillatory velocities, a second order theory is required for quantitative motion predictions. A qualitative estimate of some second order effects indicates that for specified current speeds less than one knot, the primary effect of wave-current interaction is to align the average heading angle with the current. When the wave propagation direction

relative to the current is known, oscillatory motions can then be approximated by the zero current results.

MOTION IN WAVES

EQUILIBRIUM CONDITIONS

The oscillatory motions of Moored Body Scheme A in response to sinusoidal surface waves are first determined in the absence of a current. The hull is essentially a body of revolution with a long parallel middle section, hemispherical nose, tapered afterbody and small tail appendages, as shown in Figure 1. In the following analysis the effect of the appendages is neglected. Principal dimensions and other geometric characteristics are provided in Table 1 for the body with neutral buoyancy and 60 pounds net buoyancy.

Sketches defining principal dimensions of the Moored Body Scheme A, the mooring system, and the wave train are shown in Figure 2. The body is moored beneath the surface in finite depth water to a smooth, horizontal bottom by a single cable of negligible mass. The cable is attached to the bottom of the body at an arbitrary longitudinal location. A small net buoyancy keeps the cable vertically taut and thus the body is restrained at the prescribed cable length above the bottom. The static or equilibrium cable tension is given by

$$T_s = B-W \tag{1}$$

where B and W are the buoyancy and weight of the body, respectively. It is further assumed that the longitudinal locations of the center of gravity and buoyancy relative to the cable attachment point are initially established

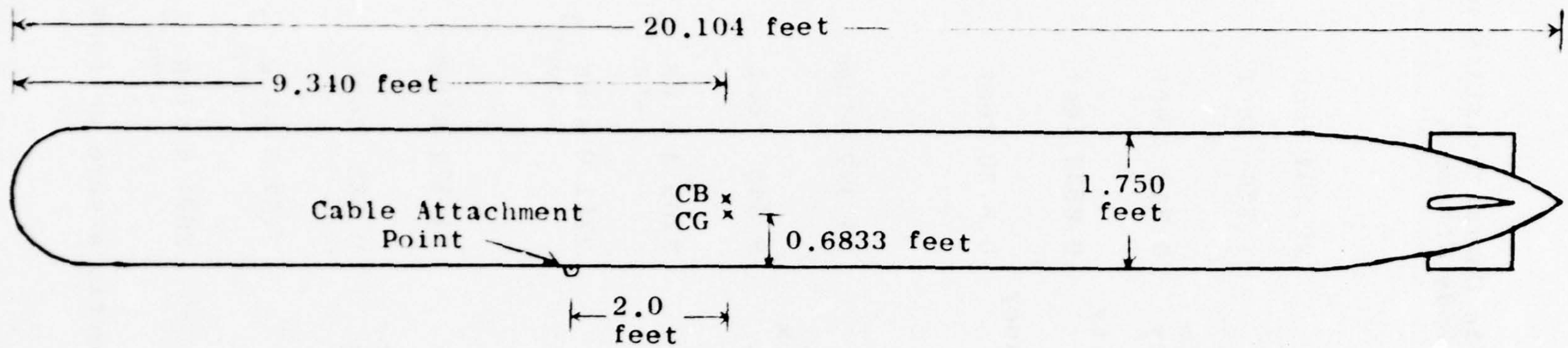

Figure 1 - Sketch of the Moored Body Scheme A

Table 1 - Geometric Characteristics of the Moored Body Scheme A

Overall length	20.104 feet	(6.1277m)
Maximum diameter	1.750 feet	(0.5334m)
Longitudinal distance from nose to center of buoyancy	9.340 feet	(2.8468m)
Height of center of gravity above baseline	0.6833 feet	(0.2083m)
Height of center of buoyancy above baseline	0.8750 feet	(0.2667m)
<u>Neutral Buoyancy</u>		
Mass	86.397 slugs	(1260.9kg)
Longitudinal distance from nose to center of gravity	9.340 feet	(2.8468m)
Moment of inertia about center of gravity*	2405.4 slug-feet^2	(3261.2kg-m^2)
Moment of inertia about y or z axis*	2751.0 slug-feet^2	(3729.9kg-m^2)
<u>Net Buoyancy 60 Pounds</u>		
Mass	84.531 slugs	(1233.6kg)
Longitudinal distance from nose to center of gravity	9.383 feet	(2.8599m)
Moment of inertia about center of gravity*	2457.3 slug-feet^2	(3331.7kg-m^2)
Moment of inertia about y or z axis*	2691.6 slug-feet^2	(3649.3kg-m^2)

*Values for moment of inertia assume uniform mass distribution

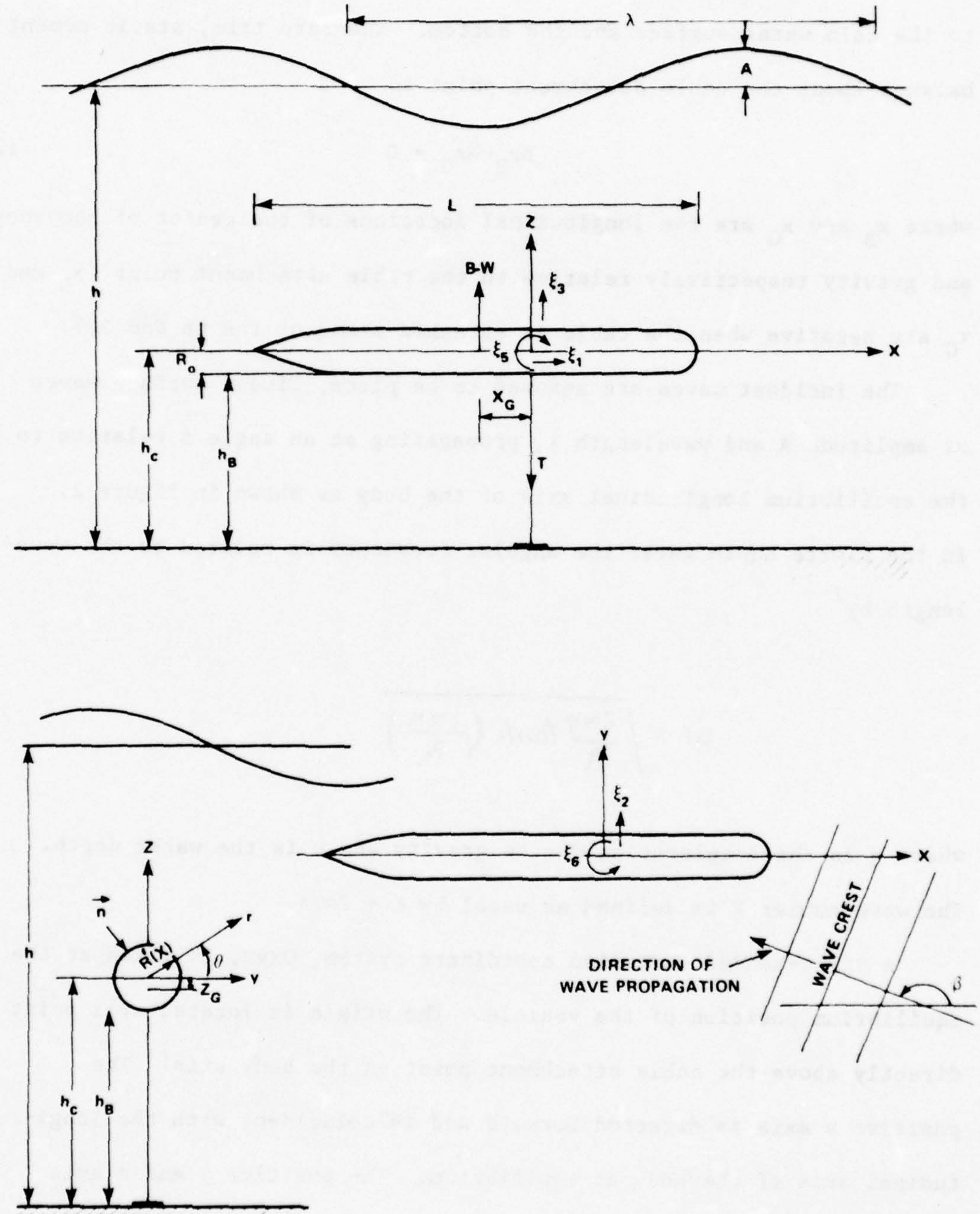

Figure 2 – Definition Sketches of Vehicle Geometry and Mooring System

such that the longitudinal axis of the body is in equilibrium parallel to the calm water surface and the bottom. The zero trim, static moment balance about the cable attachment point is

$$Bx_B - Wx_G = 0 \tag{2}$$

where x_B and x_G are the longitudinal locations of the center of buoyancy and gravity respectively relative to the cable attachment point (x_B and x_G are negative when the cable is attached ahead of the CB and CG).

The incident waves are assumed to be plane, linear surface waves of amplitude A and wavelength λ, propagating at an angle β relative to the equilibrium longitudinal axis of the body as shown in Figure 2. In the finite depth water the angular frequency is related to the wavelength by[1]

$$\omega = \sqrt{\frac{2\pi g}{\lambda} \tanh\left(\frac{2\pi h}{\lambda}\right)} \tag{3}$$

where g is the acceleration due to gravity and h is the water depth. The wave number K is defined as usual by $K = 2\pi/\lambda$.

A right-handed Cartesian coordinate system, Oxyz, is fixed at the equilibrium position of the vehicle. The origin is located at a point directly above the cable attachment point on the body axis. The positive x axis is directed forward and is coincident with the longitudinal axis of the body at equilibrium. The positive y and z axis are directed to port and upward, respectively. The polar coordinates, r' and θ, are defined in transverse sections along the length of the body, as shown in Figure 2.

In the linear analysis the oscillatory motions of the body in response to waves are expressed as small displacements and rotations from the equilibrium position (Oxyz system). Body motion in the vertical direction is assumed to be ideally restricted by the cable. The time varying displacements of the hull in the x and y directions are expressed as $\xi_1(t)$ and $\xi_2(t)$, respectively, and the angular rotations about the y and z axes by $\xi_5(t)$ and $\xi_6(t)$, respectively. Roll motion is not treated in this analysis.

EQUATIONS OF MOTION

The body is assumed to be initially at equilibrium in calm water, moored at a prescribed height off the bottom with zero trim angle. As a regular wave train passes over the water surface, oscillatory forces and moments with the same frequency as the incident wave and directly proportional to wave amplitude are developed on the body in one or all of the degrees of freedom depending on the particular wave heading angle.* The body may respond in the surge, sway, and yaw modes to the horizontal plane excitations and in the pitch mode to the vertical plane excitations. Heave motion is restricted by the cable with the oscillatory vertical force balanced by fluctuations in the cable tension. As the body responds to the wave excitations, other forces and moments, due to cable tension, inertia, and damping come into play. The equations of motion are essentially formulated in a linear, harmonic manner, although nonlinear viscous damping effects are incorporated by an equivalent linearization technique. It is assumed that body motions and tension variations are small fluctuations about equilibrium, hence,

---

[1]Milne-Thomson, "Theoretical Hydrodynamics," Fifth Edition, Macmillan Company, 1968.

*Actually, small steady and higher harmonic wave forces are also generated but are not considered in the linear theory.

only terms which depend linearly on wave amplitude and body motions are retained in the equations. It is assumed that no hydrodynamic or inertial forces act on the cable. When the wave excitations are sinusoidal functions of time, resulting body motions and tension variations are also sinusoidal with the same frequency. The wave exciting forces, body motions, and cable tension fluctuation may be written, respectively, as

$$F_i(t) = \text{Real}\left[F_{oi}\, e^{-i\omega t} \right] \tag{4a}$$

$$\xi_i(t) = \text{Real}\left[\xi_{oi}\, e^{-i\omega t} \right] \quad i \neq 3 \tag{4b}$$

$$T_3(t) = \text{Real}\left[T_{o3}\, e^{-i\omega t} \right] \tag{4c}$$

where i=1, 2, 3, 5, 6 denotes the surge, sway, heave, pitch, and yaw modes, respectively, and F_{oi} , ξ_{oi} , and T_{o3} are the complex amplitudes of the wave excitations, body displacements, and tension fluctuations, respectively.

The first order wave exciting force and moment, F_i, acting on a body of revolution submerged in finite depth water are developed in Appendix A. Three-dimensional quantities are obtained by the usual strip approximation, in which two-dimensional sectional forces are integrated over the length of the body. The formulation includes the effects of the finite depth water, the proximity of the bottom, and wave diffraction. Explicit expressions for the components of the force and moment are given in Equations (A14-a) through (A14-e) of Appendix A.

The hydrodynamic coefficients which will appear in the equations of motion, are developed in Appendix B. The added inertia coefficients, A_{ij}, associated with body acceleration, are given in Equations (B1-a) through (B1-g). The index, i, denotes the sense which the force or moment acts, and the index, j, denotes the mode of motion producing the force or moment. The added inertia coefficient for axial motion is obtained from the added mass of an equivalent spheroid, and the coefficients corresponding to transverse body motions are developed in a strip-wise fashion from potential theory, which assumes deep submergence and includes the effect of proximity to the bottom.

The damping coefficients, B_{ij}, associated with the body velocity, are given in Equations (B3-a) through (B3-i) of Appendix B. The coefficient for axial motion is derived from the submarine derivative, X_{uu}, and all of the other damping coefficients corresponding to transverse motions are obtained in a strip-wise fashion from linearized cross-flow drag considerations.

By specifying the body motions relative to the coordinate system located at a point directly above the cable attachment point on the equilibrium body axis, heave is eliminated as a possible degree of freedom. To first order, horizontal and vertical plane motions are decoupled. The surge and pitch modes are coupled[2], as are the sway and yaw motions. Tension fluctuations are contributed by the vertical wave exciting force and pitch motion. All wave exciting moments and

[2] Newman, J.N., Plaia, P., and Zarnick, E.E., "Pitching Motions of a Moored Submerged Mine in Waves," NSRDC Report 2151, March 1966.

rotational inertia and hydrodynamic coefficients are computed relative to the Oxyz axis. The equations of motion and the tension equation are then given as follows.

Surge-Pitch

The first order equations of motion for surge and pitch are

$$(m+A_{11})\ddot{\xi}_1 + B_{11}\dot{\xi}_1 + \frac{T_s}{h_B}\xi_1 + m z_G \ddot{\xi}_5 - \frac{T_s}{h_B}R_o\xi_5 = F_1(t)$$

$$(I_y + A_{55})\ddot{\xi}_5 + B_{55}\dot{\xi}_5 + \left[T_s R_o\left(1+\frac{R_o}{h_B}\right) - m z_G g\right]\xi_5$$

$$+ m z_G \ddot{\xi}_1 - \frac{T_s}{h_B}R_o\xi_1 = F_5(t)$$

where m is the mass, I_y is the moment of inertia about the y axis, A_{11} and B_{11} are, respectively, the added mass and damping for surge motion, A_{55} and B_{55} are, respectively, the added moment of inertia and moment due to damping for pitch motion and the dots above the motion variables denote, as usual, the time derivative. The third term in the surge equation is a restoring force due to cable tension. The third term in the pitch equation and the coupling terms in both equations arise due to the attachment of the cable on the keel and the vertical offset of the center of gravity from the body axis. It is assumed that any hydrodynamic coupling between the surge and pitch modes is negligible.

Using Equations (4a) and (4b) and taking appropriate time derivatives, the above equations may be written in terms of the complex amplitudes, ξ_{01} and ξ_{05} .

$$\left[-\omega^2(m+A_{11})-i\omega B_{11}+\frac{T_s}{h_B}\right]\xi_{01}+\left[-\omega^2 m z_G-\frac{T_s}{h_B}R_o\right]\xi_{05} \tag{5}$$

$$=F_{01}$$

$$\left[-\omega^2 m z_G-\frac{T_s}{h_B}R_o\right]\xi_{01}+\left[-\omega^2(I_y+A_{55})-i\omega B_{55}\right. \tag{6}$$

$$\left.+T_s R_o\left(1+\frac{R_o}{h_B}\right)-mgz_G\right]\xi_{05}=F_{05}$$

When the appropriate expressions for the excitation forces and the hydrodynamic coefficients as given in Appendices A and B are substituted, the above equations may then be solved simultaneously for the complex amplitudes of surge and pitch motion per unit wave amplitude. Substitution of ξ_{01} and ξ_{05} in Equation (4b) then provides the time varying surge and pitch motion.

Sway-Yaw

The first order equations of motion for sway and yaw motion are:

$$(m+A_{22})\ddot{\xi}_2+B_{22}\dot{\xi}_2+\frac{T_s}{h_B}\xi_2+(mx_G+A_{26})\ddot{\xi}_6+B_{26}\dot{\xi}_6$$

$$=F_2(t)$$

$$(I_z+A_{66})\ddot{\xi}_6 + B_{66}\dot{\xi}_6 + (mx_G+A_{62})\ddot{\xi}_2 + B_{62}\dot{\xi}_2 = F_6(t)$$

where I_z is the moment of inertia in yaw, A_{22} and B_{22} are, respectively, the added mass and damping for sway motion, A_{66} and B_{66} are, respectively, the added moment of inertia and moment due to damping for yaw motion, A_{26} and A_{62} are added inertia coupling coefficients and B_{26} and B_{62} are damping coupling coefficients. The third term in the sway equation is a restoring force due to the cable tension. The choice of the coordinate system at a point above the cable attachment has eliminated any cable restoring moment in the yaw equation. Coupling is a result of both inertial and hydrodynamic effects in these modes.

In terms of the complex amplitudes, ξ_{02} and ξ_{06}, the equations of motion are written as

$$\left[-\omega^2(m+A_{22}) - i\omega B_{22} + \frac{T_s}{h_B}\right]\xi_{02} + \left[-\omega^2(mx_G+A_{26}) - i\omega B_{26}\right]\xi_{06} = F_{02} \tag{7}$$

$$\left[-\omega^2(mx_G+A_{62}) - i\omega B_{62}\right]\xi_{02} + \left[-\omega^2(I_z+A_{66}) - i\omega B_{66}\right]\xi_{06} = F_{06} \tag{8}$$

where the excitation forces and hydrodynamic coefficients are given in Appendices A and B.

Cable Tension

In order that the body be completely restrained against heave motion, it is required that the total cable tension, which is the sum of the static and oscillatory components, be greater than zero and less than a value which would snap the cable at any instant of time.

$$0 < T_s + T_3(t) < T_{Snap} \qquad (9)$$

If the total tension drops to zero, the cable slackens and the body may move downward. During a later portion of the wave cycle, the body will move upward again, and a large impulsive force on the cable can be generated as the cable becomes taut.

Within the limits of Equation (9), the vertical force must be balanced by both the static and time varying components of the cable tension. Statically, the balance is provided by Equation (1). The oscillatory component is given by

$$T_3 = F_3 - [-mx_G + A_{35}]\ddot{\xi}_5 - B_{35}\dot{\xi}_5$$

and in terms of the complex amplitudes

$$T_{03} = F_{03} + [\omega^2(-mx_G + A_{35}) + i\omega B_{35}]\xi_{05} \qquad (10)$$

where A_{35} and B_{35} are the added inertia and damping providing a vertical

force due to pitch motion. Equation (9) requires that

$$|\Gamma_{03}| < T_s \text{ or } (T_{snap} - T_s) \quad \text{, whichever is smaller.} \qquad (11)$$

NONLINEAR DAMPING AND THE SOLUTION OF THE EQUATIONS

The restoring forces and moments affecting the moored body can introduce resonant motion when the damping is small. As is typical for a linear system, the amount of damping determines the magnitude of the motion near the resonant frequency. The primary source of damping for a deeply submerged, oscillating body is the nonlinear viscous drag, and although this force may be small, it can be of significance if a motion resonance occurs in the frequency range of excitation. In Appendix B a method is shown whereby the nonlinear viscous drag is approximated by a pseudo-linear function of velocity which may be incorporated in the linear equations of motion. The damping coefficients, B_{ij}, remain amplitude dependent, however, and the equations of motion are solved by an iterative procedure.

When the equations of motion are strictly linear, that is, all of the coefficients are functions of frequency only, solutions are ordinarily obtained in the form of response amplitude operators, which are the motion amplitudes per unit wave amplitude, $|\xi_{oi}|/A$. The response amplitude operators are independent of wave amplitude, and the absolute amplitude of motion, $|\xi_{oi}|$, is obtained by multiplying the response by an arbitrary wave amplitude. In the case where the damping coefficients are amplitude dependent, solutions may be obtained

in the form of a response amplitude operator, except that $|\xi_{oi}|/A$ is no longer independent of wave amplitude.

From Appendix B, the equivalent pseudo-linear form for the damping coefficients is given by

$$B_{ij} = \frac{8}{3\pi} \rho \, G_{ij} \, \omega \, |\xi_{oj}| \, C_D$$

where the G_{ij}'s are constants depending upon geometry and mode of motion, as shown in Equations (B3-a) through (B3-i). In terms of the motion per unit wave amplitude, $|\xi_{oi}|/A$, the damping coefficient is

$$B_{ij} = \frac{8}{3\pi} \rho \, G_{ij} \, \omega \left(\frac{|\xi_{oj}|}{A}\right) C_D A$$

In the iterative method used to solve the equations of motion, initial values for the damping coefficients B_{ij} are determined from initial arbitrary choices for $|\xi_{oj}|/A$ with a given value for the wave amplitude, A. These coefficients are then substituted into the equations of motion, which are solved for new values of $|\xi_{oj}|/A$. The new motion responses are then used to redefine the damping coefficients, and the process is repeated until a convergent solution is obtained. Since the damping coefficient is a function of wave amplitude, a distinct response, $|\xi_{oj}|/A$, is determined for each specified wave amplitude.

The damping term appearing in the equations of motion is also proportional to C_D, the crossflow drag coefficient for a circular cylinder. This coefficient is difficult to estimate since it is to

some extent an unknown function of Reynolds number, wave frequency, and amplitude. The coefficient may vary from 0.4 to 1.2 depending on whether the flow is completely turbulent or laminar.

In the following theoretical results, the product, $C_D A$, has been retained as an arbitrary constant which determines the magnitude of the damping coefficient. It is understood that C_D and A may each be varied independently within appropriate limits.

An example of the resonant motion and the effect of nonlinear damping on the Moored Body Scheme A is shown in Figure 3. The pitch amplitude per unit wave amplitude in degrees per foot is plotted versus excitation wavelength. The body is moored by a 20-foot cable at a point 2 feet ahead of the center of gravity. The water depth is 120 feet, the wave heading angle is 180 degrees, and the static tension is 60 pounds.

A pitch resonance occurs at a wavelength of about 1100 feet, which according to Equation (3) corresponds to an angular frequency of 0.325 radians/sec. The family of curves at the resonance corresponds to different values for the product, $C_D A$. Away from resonance, the curves in the family merge into a single curve, thus indicating the significance of the damping only about resonance.

From Figure 3, the peak magnitude of resonance may be plotted against $C_D A$. As shown in Figure 4 the response at resonance is roughly proportional to the inverse square root of the damping factor, $C_D A$. The absolute value of pitch motion has then been plotted against wave amplitude for different choices of C_D, and this is shown in Figure 5.

Other modes of motion would be similarly affected about resonance by a damping variation, however, the surge, sway, and yaw resonances

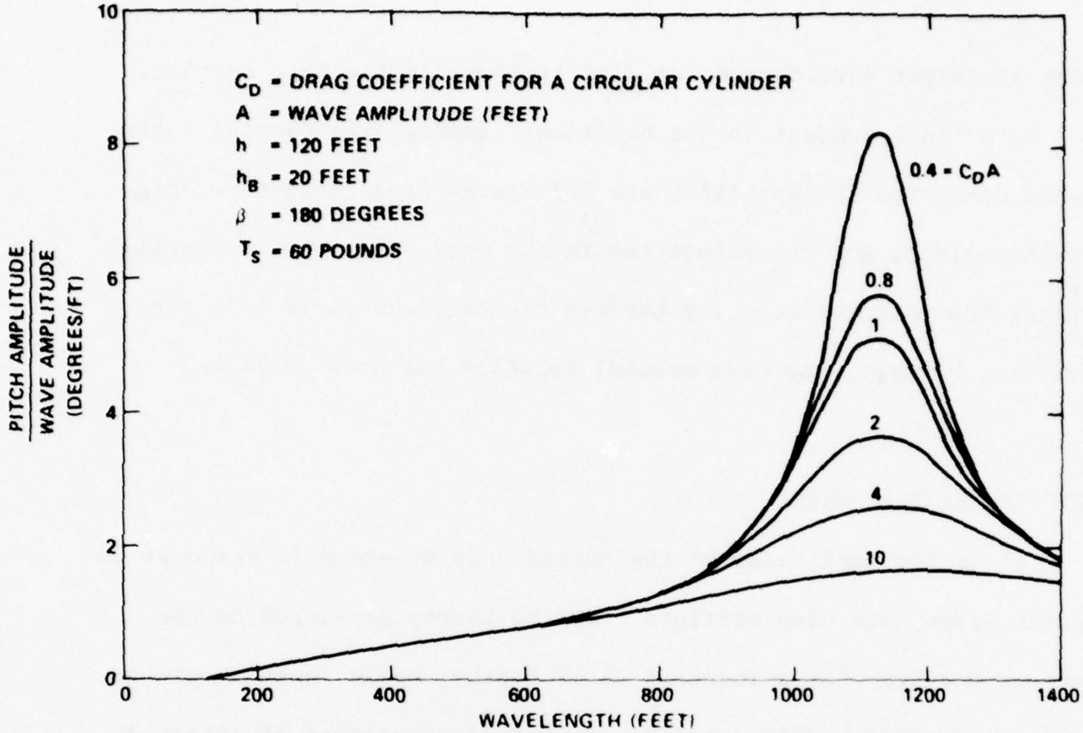

Figure 3 – Effect of Non-linear Damping on Pitch Response in Regular Waves

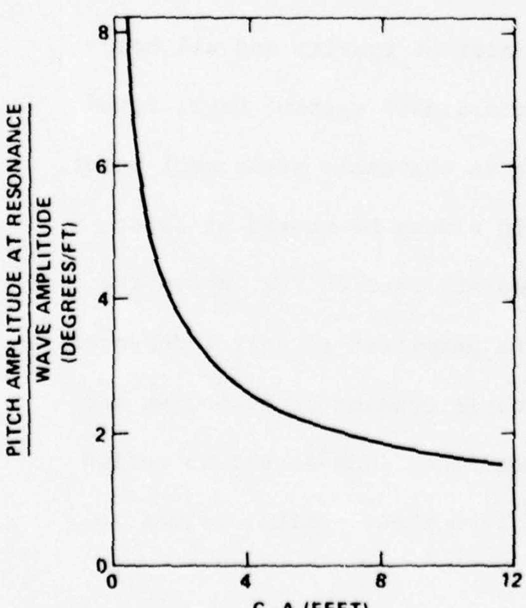

Figure 4 – Effect of Damping on the Peak Magnitude of the Pitch Response at Resonance in Regular Waves

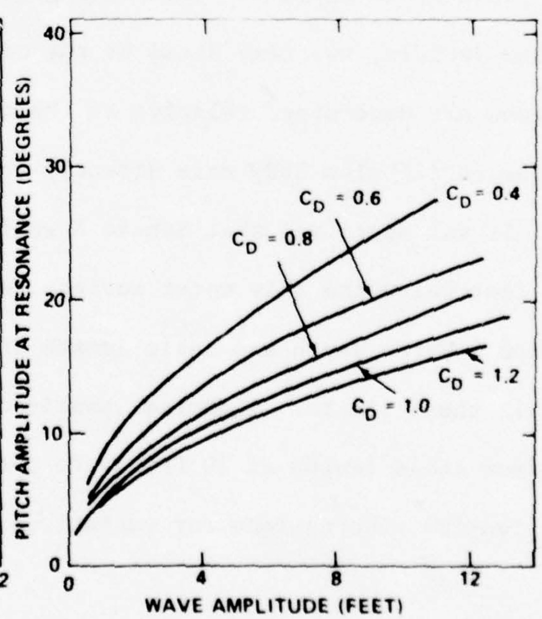

Figure 5 – Effect of Wave Amplitude and Drag Coefficient on Pitch Angle at Resonance in Regular Waves

occur at longer wavelengths, as will be shown in the next section.

As a final comment on the nonlinear damping, the damping coefficients developed in Appendix B are formulated from cross-flow drag considerations, and the velocities in the drag terms should ideally reflect the relative velocity between the body and fluid. In the analysis, however, the wave orbital velocity has been neglected.

MOTION IN REGULAR WAVES

The motion amplitudes of the Moored Body Scheme A in response to regular waves have been obtained from the theory developed in the previous section for a range of water depths, cable lengths, static tensions and wave heading angles. Principal dimensions of Scheme A are provided in Table 1. The mooring cable is attached to the keel of the vehicle, two feet ahead of the center of gravity and all body motions are determined relative to the coordinate system, Oxyz, fixed on the equilibrium body axis directly above the cable attachment point.

It was specified that Scheme A would always be moored at least 100 feet below the calm water surface and at least 20 feet above the bottom. Water depth and cable length are permitted to vary independently within these limits. A nominal static cable tension of 60 pounds and minimum cable length of 20 feet were specified. The effect on motion and tension fluctuations for variations from these nominal values is

also examined.

The presence of restoring forces and moments in the equations of motion means that resonances will be introduced in the motion responses. The natural frequencies for the various modes are given by

$$\omega_{surge} = \sqrt{\frac{T_s/h_B}{m + A_{11}}} \qquad \omega_{sway} = \sqrt{\frac{T_s/h_B}{m + A_{22}}}$$

$$\omega_{pitch} = \sqrt{\frac{T_s R_e (1 + R/h_B) - m g z_G}{I_y + A_{55}}}$$

The natural frequencies are tabulated in Table 2 for different values of the static cable tension, cable length, and vertical center of gravity.

Coupling between the modes also means that a resonance in one mode may be evident in another mode. This is particularly true of the sway-yaw modes. Although the yaw equation contains no restoring moment, the strong coupling due to inertial and hydrodynamic effects means that the sway resonance is significantly reflected in the yaw response. The pitch resonance is also reflected to some degree in the tension response. Coupling between the surge and pitch modes is relatively weak although the surge resonance can affect the pitch response if the cable length becomes very small.

At frequencies less that about 0.25 radians/sec resonances are of little consequence in a real seaway condition, since there is little energy below this frequency even in severe sea states. From Table 2 for a

Table 2 - Resonant Frequencies of the Moored Body Scheme A

Static Cable Tension in feet	Cable Length in feet	Vertical Center of Gravity in feet	Resonant Frequencies in radians/second		
			Pitch	Surge	Sway-Yaw
60	10	-0.1917	0.326	0.266	0.187
"	20	"	0.325	0.188	0.132
"	50	"	0.325	0.119	0.084
"	∞	"	0.325	0.0	0.0
120	10	-0.1917	0.340	0.381	0.266
"	20	"	0.339	0.269	0.188
"	50	"	0.338	0.170	0.119
"	∞	"	0.338	0.0	0.0
20	10	-0.1917	0.317	0.153	0.108
"	20	"	0.316	0.108	0.076
"	50	"	0.316	0.068	0.048
"	∞	"	0.316	0.0	0.0
60	20	-0.1917	0.325	0.188	0.132
"	"	-0.2000	0.332	0.188	0.132
"	"	-0.1500	0.292	0.188	0.132
"	"	-0.2500	0.368	0.188	0.132

nominal static tension of 60 pounds and cable length greater than 20 feet, pitch is the only mode where resonant motion is significantly excited by a real seaway.

Figures 6 through 10 show the effect on the motion and tension responses of water depth variation with constant depth of submergence. The amplitude of motion or tension per unit wave amplitude is plotted as a function of excitation wavelength. The water depth is increased from 120 to 400 feet and the cable length is correspondingly increased from 20 to 300 feet such that a 100-foot submergence depth is maintained. The minimum submergence depth (100 feet) regardless of water depth provides a worst case condition for all quantities. As indicated in the figures, the 120-foot water depth is a worst case for surge, sway, and yaw motion, and the 400-foot depth (essentially infinite depth) is a worst case for pitch and tension fluctuations.

The responses were obtained with a nominal static cable tension of 60 pounds. Surge and pitch motions are maximum in head waves (β=180 degrees); sway and yaw motions are maximum in beam waves (β=90 degrees), so results are provided only for these heading angles. Tension fluctuations are mostly unaffected by heading angle.

Except for surge, which is given for the zero damping case, the responses for the other modes of motion were obtained for the damping factor, $C_D A=1.0$. With the exception of pitch, all resonances occur at very long wavelengths (low frequencies), and hence the damping variation is not of great significance in the wavelength range indicated in the figures. The effect of damping variation for pitch motion is shown in Figure 3.

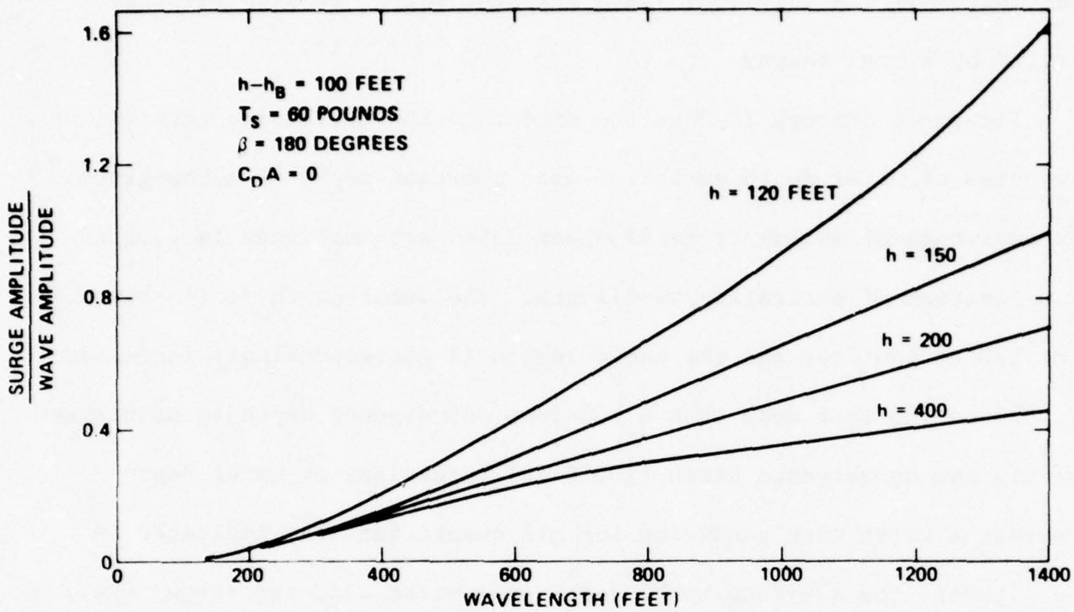

Figure 6 – Effect of Water Depth on Surge Motion in Regular Waves

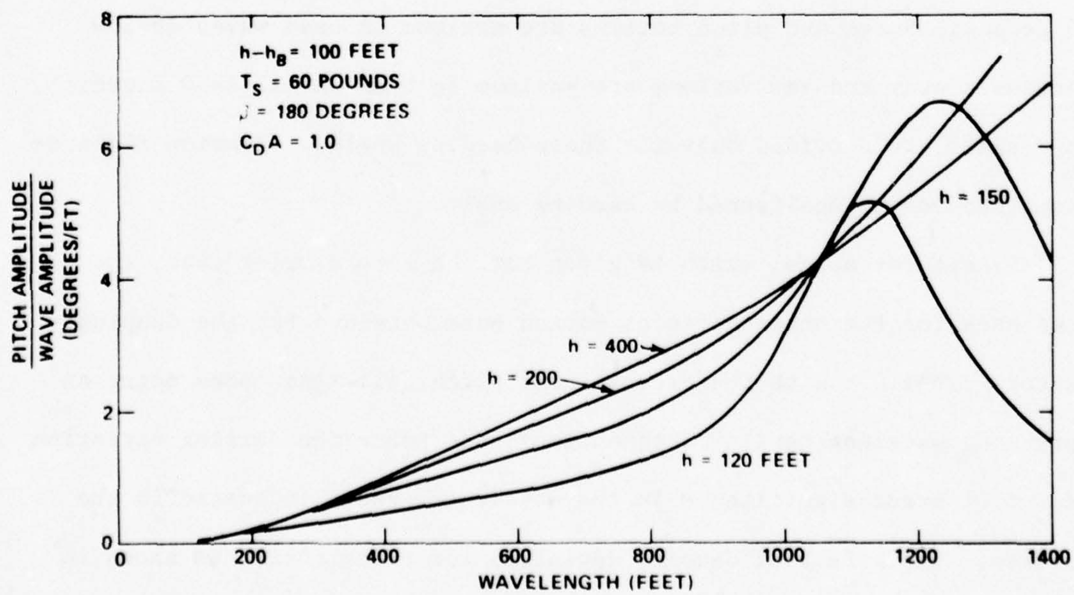

Figure 7 – Effect of Water Depth on Pitch Motion in Regular Waves

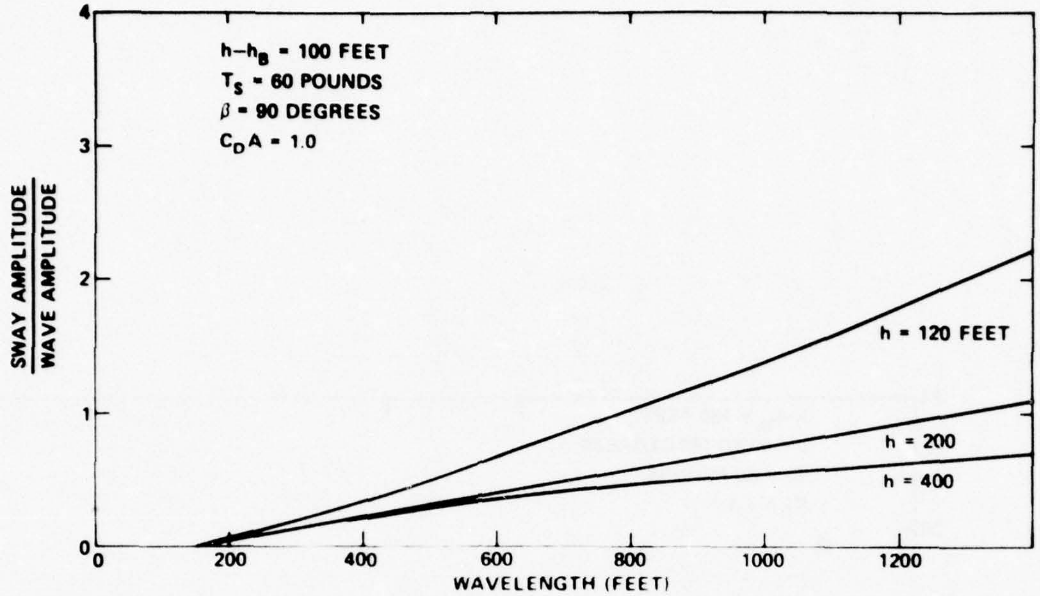

Figure 8 – Effect of Water Depth on Sway Motion in Regular Waves

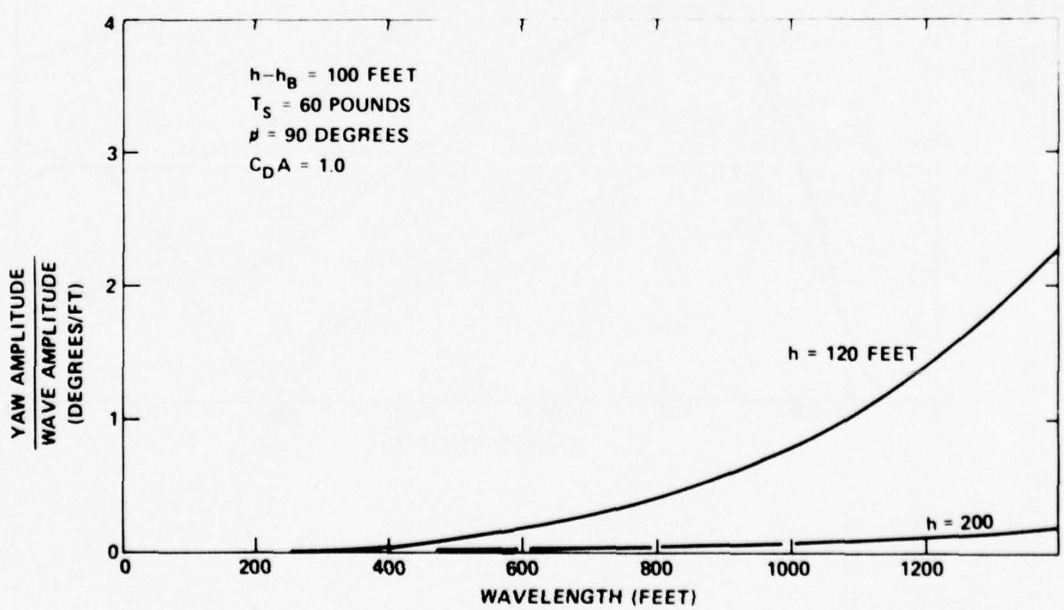

Figure 9 – Effect of Water Depth on Yaw Motion

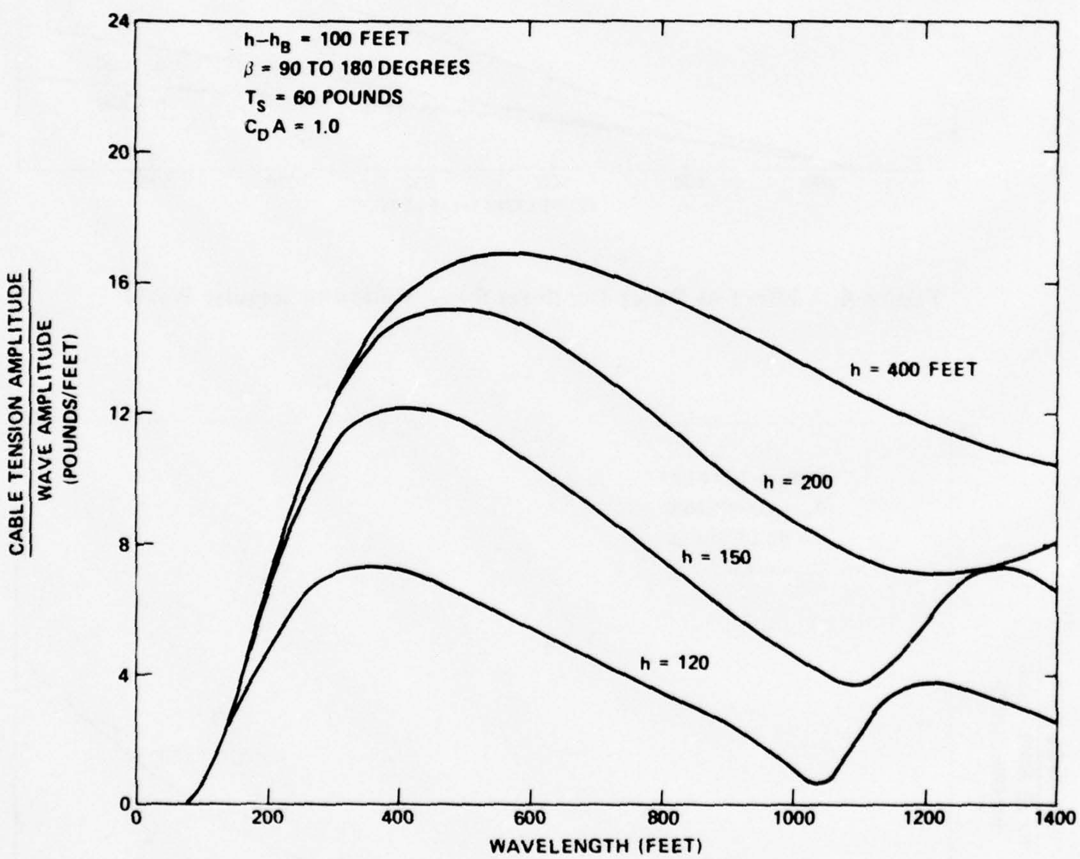

Figure 10 – Effect of Water Depth on Tension in Regular Waves

From Table 2 the pitch resonant frequency remains essentially unchanged as cable length increases. Due to the increased water depth, however, the resonance is shifted toward longer wavelengths, as noted in Figure 7. In fact, the peak for the 200 and 400-foot depths are shifted beyond the wavelength range shown. The cable length increase does shift the surge, sway, and yaw resonances to lower frequencies, and these peaks are well beyond the wavelength range shown in Figures 6, 8, and 9. The tension responses are shown in Figure 10. Tension is primarily determined by the vertical wave excitation force, although some coupling from pitch motion is evident at the pitch resonant wavelength.

Figures 11 through 15 show the effect of cable length variation at a constant water depth of 120 feet and nominal static cable tension of 60 pounds. All responses, except surge, were obtained with the damping factor, C_DA=1.0. Generally, as the cable length increases, pitch motion and tension fluctuations increase, and horizontal plane motions decrease with the resonance being shifted to lower frequencies.

Figures 16 through 19 show the effects of static cable tension variation for constant water depth of 120 feet and cable length of 20 feet. As before, all responses, except surge, were obtained with a damping factor C_DA=1.0. An increase in the static tension shifts all resonances towards higher frequencies and thus increases the motion amplitudes at frequencies above resonance. In the first order theory, tension fluctuations are relatively unaffected by the static tension and, hence, are not shown.

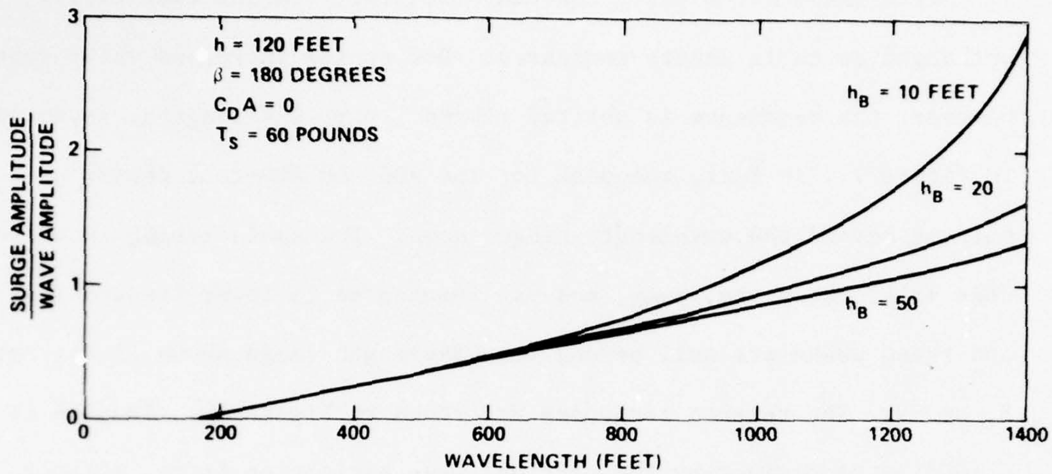

Figure 11 – Effect of Cable Length on Surge Motion in Regular Waves

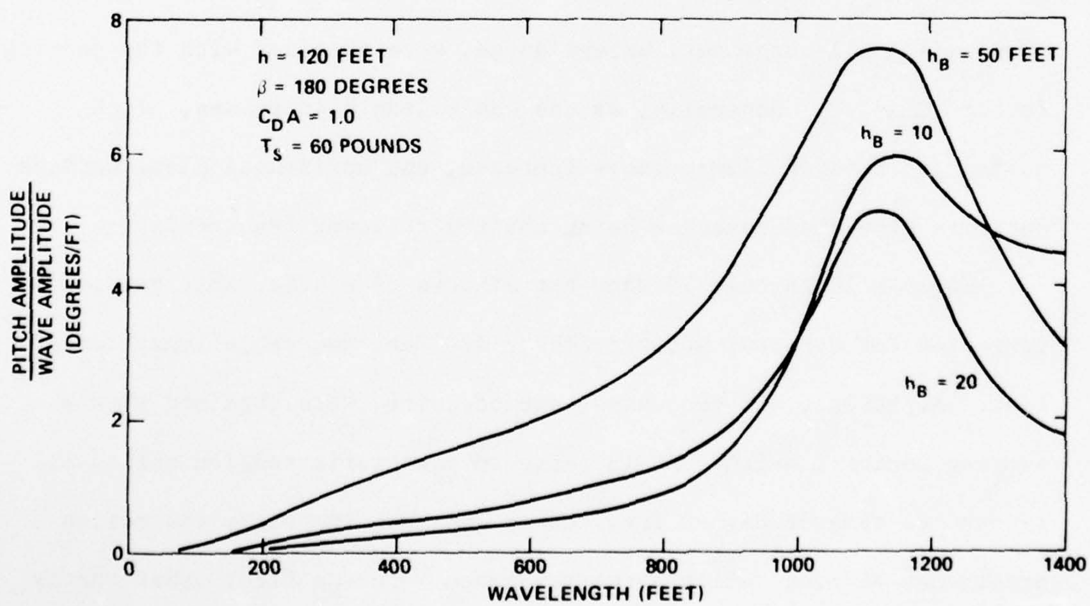

Figure 12 – Effect of Cable Length on Pitch Motion in Regular Waves

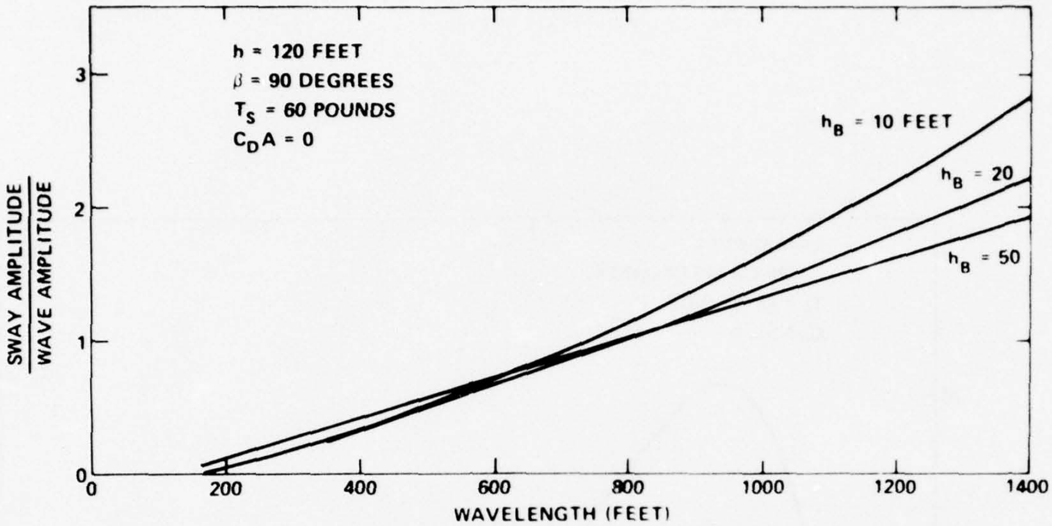

Figure 13 – Effect of Cable Length on Sway Motion in Regular Waves

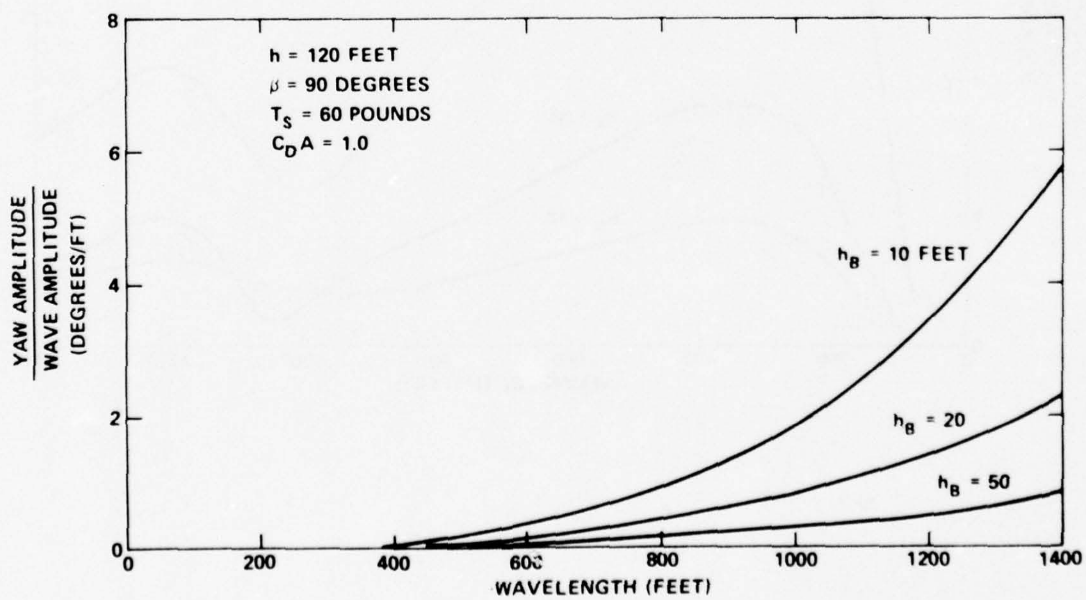

Figure 14 – Effect of Cable Length on Yaw Motion in Regular Waves

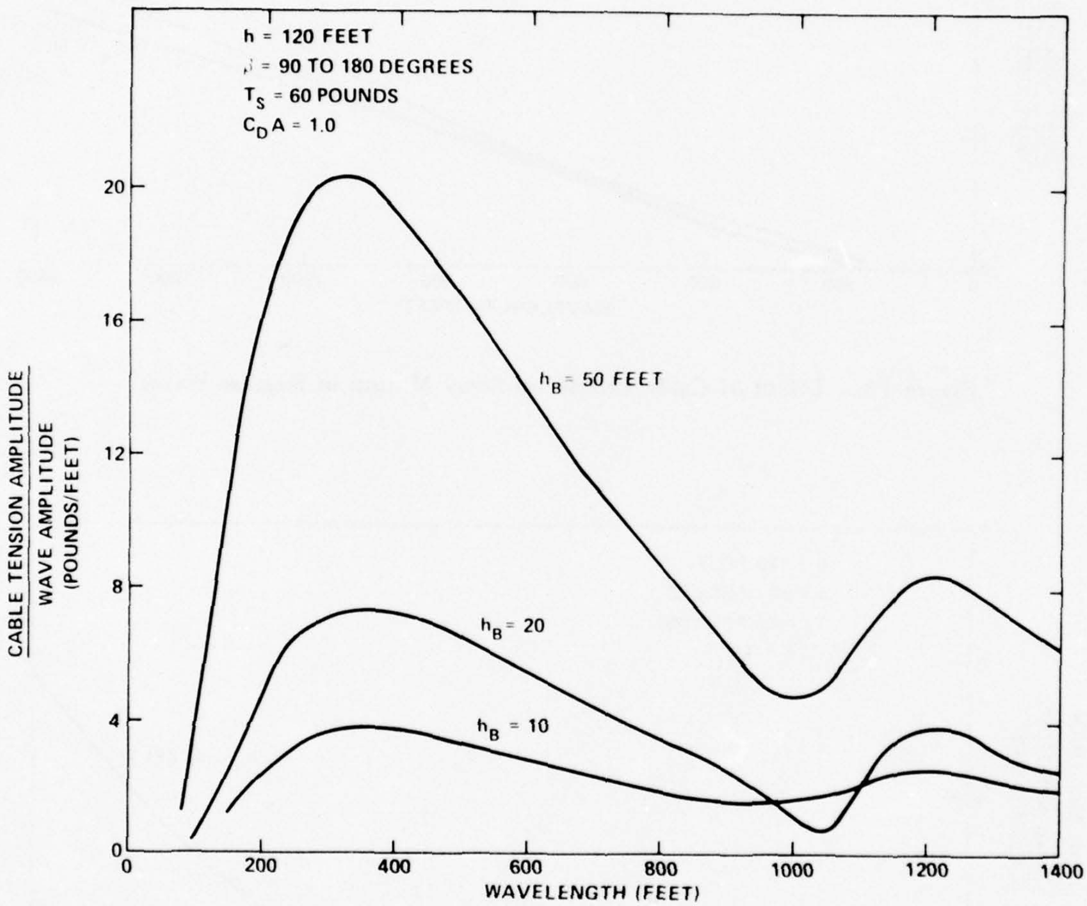

Figure 15 – Effect of Cable Length on Tension in Regular Waves

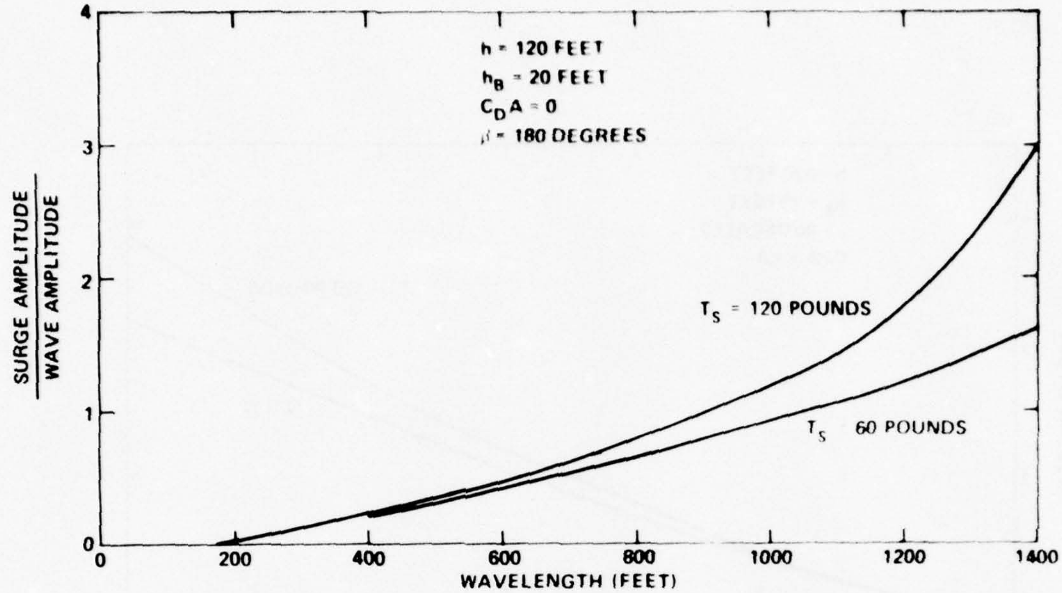

Figure 16 – Effect of Static Cable Tension on Surge Motion in Regular Waves

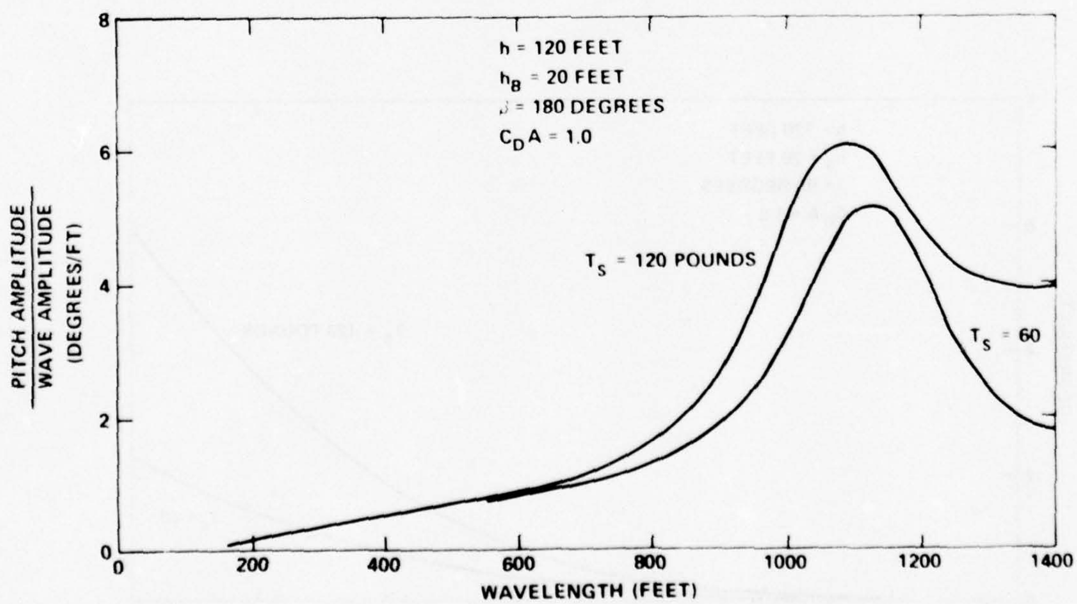

Figure 17 – Effect of Static Cable Tension on Pitch Motion in Regular Waves

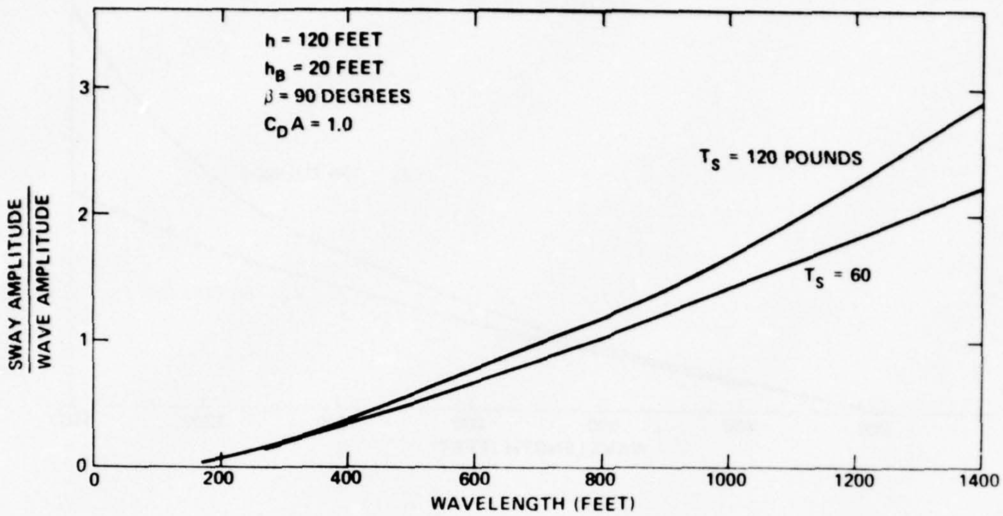

Figure 18 – Effect of Static Cable Tension on Sway Motion in Regular Waves

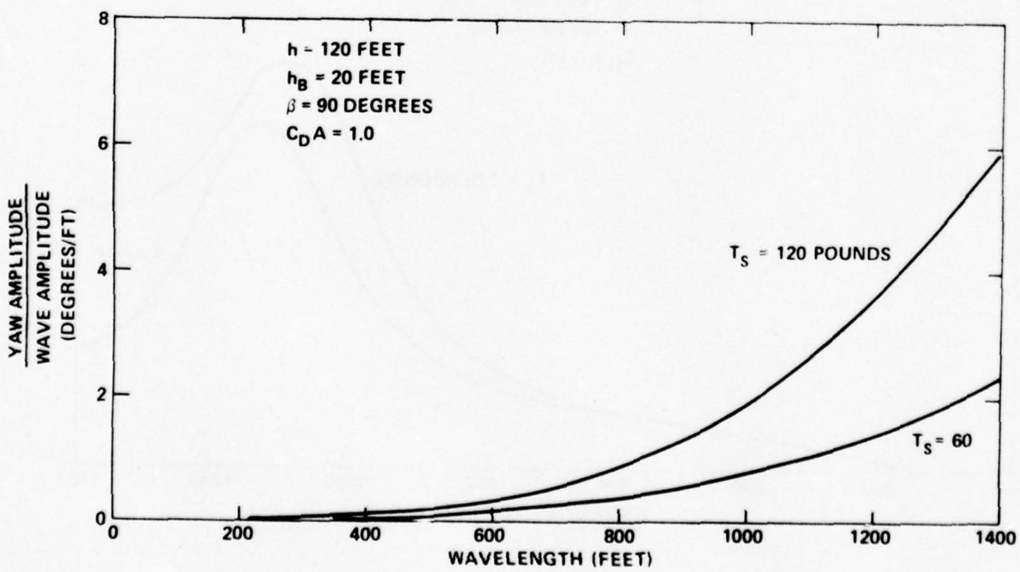

Figure 19 – Effect of Static Cable Tension on Yaw Motion in Regular Waves

The motion responses shown in Figures 6 through 19 are independent of wave amplitude, except around the resonances, and the pitch motion is the only mode in which the resonant frequency is really high enough to fall well within the range of realistic wave excitation. It is required, however, that the absolute amplitudes of the motion and hence, wave amplitude, are small enough such that the basic linear assumptions of the formulation are satisfied. For example, surge or sway amplitudes which are greater than 10 feet when the cable length is only 20 feet would be approaching unacceptable limits of the linear theory.

Roughly, the linear theory is expected to provide reliable results when the amplitude of the cable deflection angle from the vertical and the pitch and yaw angle amplitudes are less than 30 degrees.

As mentioned previously, a condition of the linear formulation is that the tension fluctuation be small compared to the static cable tension. With a static tension of 60 pounds, this condition is clearly marginal. As an example, consider the amplitude of tension fluctuations as given by Figure 10 for the 400-foot water depth and wavelength of about 600 feet. The tension fluctuation response is about 17 pounds/foot, and for a wave of even a few feet amplitude the absolute amplitude of the tension fluctuation is of the order of the static tension. Furthermore, the wave amplitude does not have to be very large before the vertical restraint condition of Equation (11) is violated.

The static cable tension could be increased to relieve this situation, however, this would also have the adverse effects of shifting all of the motion resonances towards higher frequencies, as indicated in Table 2.

The fact that tension fluctuations may not necessarily be small compared to the static tension for the conditions specified in this analysis is a limitation of the linear analysis. The large tension fluctuations can introduce harmonic components into the motion responses, however, a consistent second order theory would be required to quantitatively predict the effect.

MOTION IN A SEAWAY

A statistical representation of the motions of Scheme A in irregular seas may be determined in a manner following the procedure of St. Denis and Pierson[3] and summarized by Frank and Salvesen[4]. Briefly, with the assumptions of stationary, Gaussian processes for the wave excitations and motion responses, the energy associated with the response of the body in random waves may be represented by the linear superposition of responses to a number of sinusoidal waves.

The significant amplitude of motion in a particular mode is given by

$$A_{1/3} = 2\left[\int_0^\infty [R_s(\omega)]^2 S(\omega)\, d\omega\right]^{1/2} \tag{12}$$

where $R_s(\omega)$ is the amplitude of the response in a given mode to a sinusoidal wave of unit amplitude, and $S(\omega)$ is the energy in the sea which is associated within an infinitesimal frequency band at the frequency, ω. In this analysis, it has been assumed that the seaway is unidirectional and fully developed, and can therefore be statistically described by the one parameter, Pierson-Moskowitz Spectrum[3] of the form

$$S(\omega) = \frac{A_o}{\omega^5} e^{-\frac{B_o}{\omega^4}} \qquad (13)$$

where A_o=0.0081g^2, B_o=33.561/$h_{1/3}^{2}$, and $h_{1/3}$ is the significant waveheight in feet. A plot of the Pierson-Moskowitz Spectrum (Equation (13)) is shown in Figure 20 for several values of $h_{1/3}$. Other characteristics of the Spectrum are given in Table 3[4]. The significant waveheight is the average of the highest one-third of the waves and is a measure of the sea state. Subject to the condition of linear waves, it is assumed that the Pierson-Moskowitz Spectrum, as given in Equation (13), is independent of water depth, although the relationship between frequency and wavelength given by Equation (3) is still applicable.

The method just outlined to determine the statistical motion in irregular waves is applicable for strictly linear responses. For a given response amplitude operator, which is independent of wave amplitude, and a specified sea spectrum, the significant amplitude of motion is uniquely defined for a given significant waveheight. In the present analysis the nonlinear damping and pseudo-linearization technique used to solve the equations of motion result in motion responses which are amplitude dependent near resonances. However, even though the response amplitude operators are not uniquely defined independent of wave amplitude,

---

[3] St. Denis, M. and W.S. Pierson, "On the Motion of Ships in Confused Seas," Trans. SNAME, Vol. 61, 1953.

[4] Frank, W. and N. Salvesen, "The Frank Close-Fit Ship-Motion Computer Program," NSRDC Report No. 3289, June 1970.

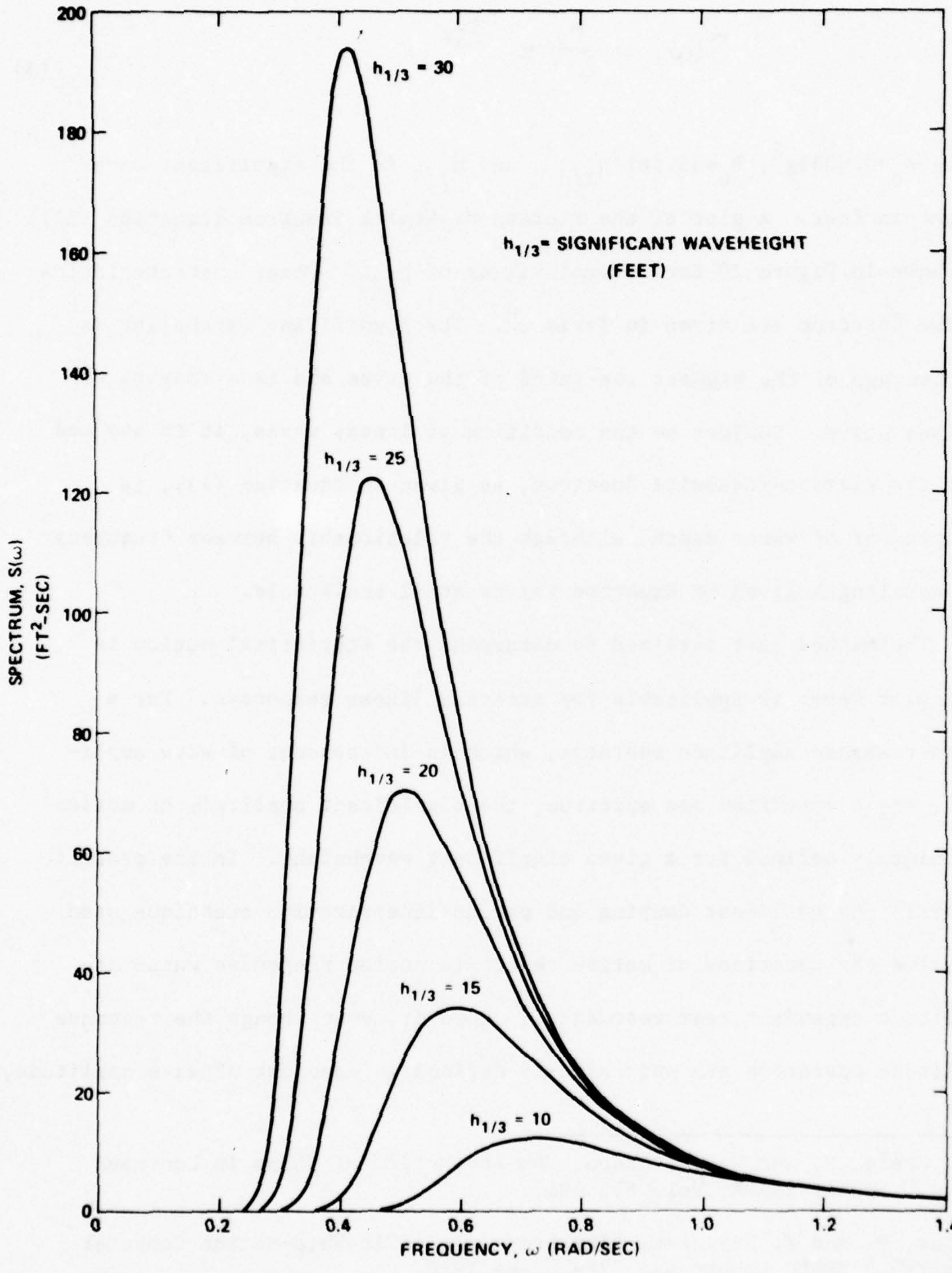

Figure 20 – Pierson-Moskowtiz Sea Spectrum

Table 3 - The Pierson-Moskowitz Sea Spectrum

Sea State	Significant Wave Height ft	Significant Range of Periods sec	Percent of Maximum Energy sec	Average Period sec	Average Wave Length ft
0	0.10	0.34 - 1.09	0.87	0.62	1.31
0	0.15	0.42 - 1.33	1.07	0.76	1.97
1	0.50	0.77 - 2.43	1.95	1.39	6.57
1	1.00	1.09 - 3.43	2.76	1.96	13.14
1	1.20	1.19 - 3.76	3.02	2.15	15.76
2	1.50	1.34 - 4.21	3.38	2.40	19.70
2	2.00	1.54 - 4.86	3.90	2.77	26.27
2	2.50	1.72 - 5.43	4.36	3.10	32.84
2	3.00	1.89 - 5.95	4.78	3.40	39.41
3	3.50	2.04 - 6.43	5.16	3.67	45.98
3	4.00	2.18 - 6.87	5.52	3.92	52.54
3	4.50	2.31 - 7.29	5.86	4.16	59.11
3	5.00	2.44 - 7.68	6.17	4.38	65.68
4	6.00	2.67 - 8.41	6.76	4.80	78.82
4	7.00	2.89 - 9.09	7.30	5.19	91.95
4	7.50	2.99 - 9.41	7.56	5.37	98.52
5	8.00	3.08 - 9.71	7.81	5.55	105.09
5	9.00	3.27 -10.30	8.28	5.88	118.22
5	10.00	3.45 -10.86	8.73	6.20	131.36
5	12.00	3.78 -11.90	9.56	6.79	157.63
6	14.00	4.08 -12.85	10.33	7.34	183.90
6	16.00	4.36 -13.74	11.04	7.84	210.17
6	18.00	4.63 -14.57	11.71	8.32	236.45
6	20.00	4.88 -15.36	12.34	8.77	262.72
7	25.00	5.45 -17.17	13.80	9.80	328.40
7	30.00	5.97 -18.81	15.12	10.74	394.08
7	35.00	6.45 -20.32	16.33	11.60	459.76
7	40.00	6.90 -21.72	17.46	12.40	525.43
8	45.00	7.32 -23.04	18.52	13.15	591.11
8	50.00	7.71 -24.28	19.52	13.87	656.79
8	55.00	8.09 -25.47	20.47	14.54	722.47
8	60.00	8.45 -26.60	21.38	15.19	788.15
9	70.00	9.12 -28.73	23.09	16.41	919.91
9	80.00	9.75 -30.72	24.69	17.54	1050.87
9	90.00	10.35 -32.58	26.19	18.60	1182.23
9	100.00	10.91 -34.34	27.60	19.61	1313.59

we may use the statistical method to define an envelope for the significant motion and tension amplitudes. As shown in Figure 3, the product C_DA provides limits on the statistical amplitudes at each significant waveheight.

The response amplitude operators like those shown in Figures 6 through 19, together with the Pierson-Moskowitz Sea Spectrum, as defined in Equation (13), have been used in Equation (12) to obtain the significant amplitude of the motions and tension fluctuation as a function of significant waveheight (sea state). Results are shown in Figures 21 through 32 for the various water depth, cable length, and heading angle conditions previously considered. In all cases, the static cable tension was 60 pounds. With the exception of surge, results were obtained with damping factor limits of $0.2 \leq C_DA \leq 2.0$. The envelope defined by these limits is indicated by the shaded region in the figures. Surge results are shown only for the zero damping case, since in practice damping in this mode is very small. Response amplitude operators were computed between frequencies of 0.25 and 1.4 radians/sec. As shown in Figure 20, for significant waveheights less than 30 feet, virtually all of the wave energy is contained in this range.

Figure 21 shows the significant amplitude of pitch obtained with response amplitude operators defined for the various values of the damping coefficients, C_DA. For sea states with significant waveheight less than about 17 feet the spectral density at low frequencies (long wavelengths) is insignificant and, hence, resonant motion is not excited. In higher sea states the spectral density at lower frequencies is no longer

negligible, and the long waves tend to generate motion about the resonance where the response is amplitude dependent. Reasonable limits for the damping factor may then be regarded as defining an envelope for the statistical motion amplitudes. Figures 23 and 28 show the pitch envelope for water depth and cable length variations within the range, $0.2 < C_D A < 2.0$.

Figures 24, 25, 29, and 30 show the significant amplitudes for sway and yaw. Envelopes for these modes are much narrower than the pitch, since the resonances occur at very low frequencies and within this range of excitation there is very little change in the response amplitude operators due to the damping variation.

In Figures 22 and 27 are shown the significant amplitude of surge motion. These results indicate no envelope since only the zero damping response amplitude operator was used.

Figures 26 and 31 show the significant amplitude of the tension fluctuations. These responses are relatively unchanged by the damping variation, which would appear only through pitch coupling.

Figure 32 shows the effect of heading angle on the various motion and tension significant amplitudes. A significant waveheight of 25 feet was chosen and the shaded region indicates the damping factor limits $0.2 \leq C_D A \leq 2.0$.

At high sea states the significant amplitudes of motion shown in Figures 21-32 indicate magnitudes which exceed the valid range of the linear theory. In particular a condition for the linear formulation of the equations of motion and restraint of the body in the heave mode is that the cable tension fluctuations not exceed the static cable tension (Equation (11)). Figure 26 shows that in a seaway the signficant

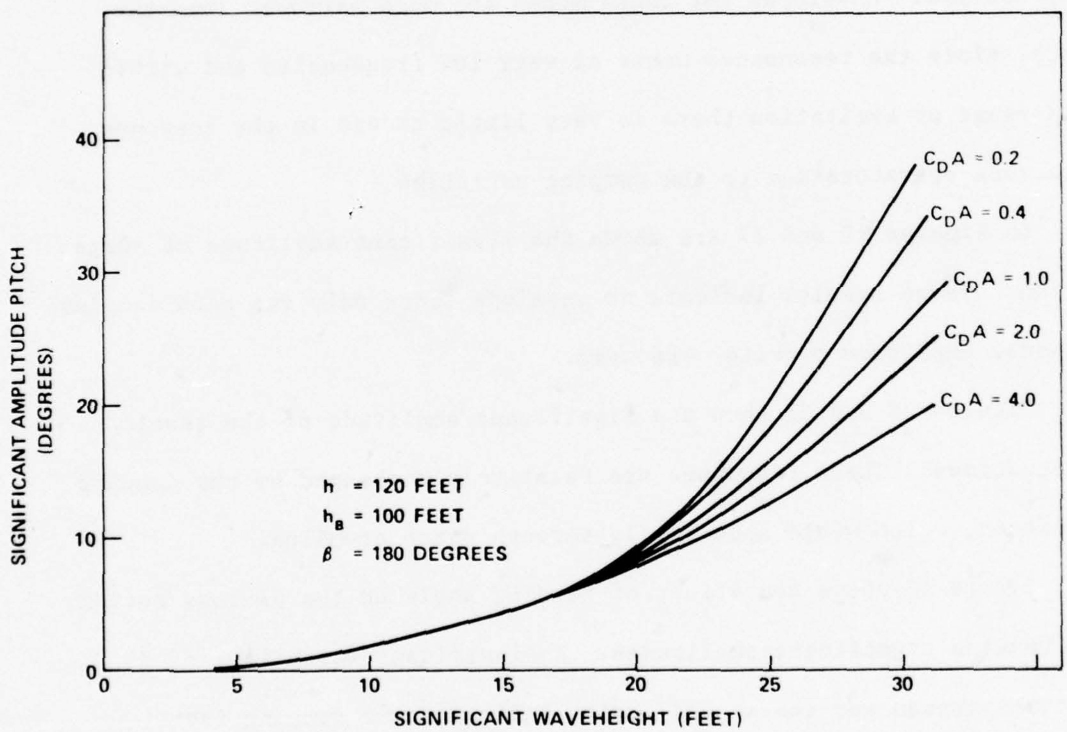

Figure 21 – Effect of Damping on Pitch Motion in Irregular Waves

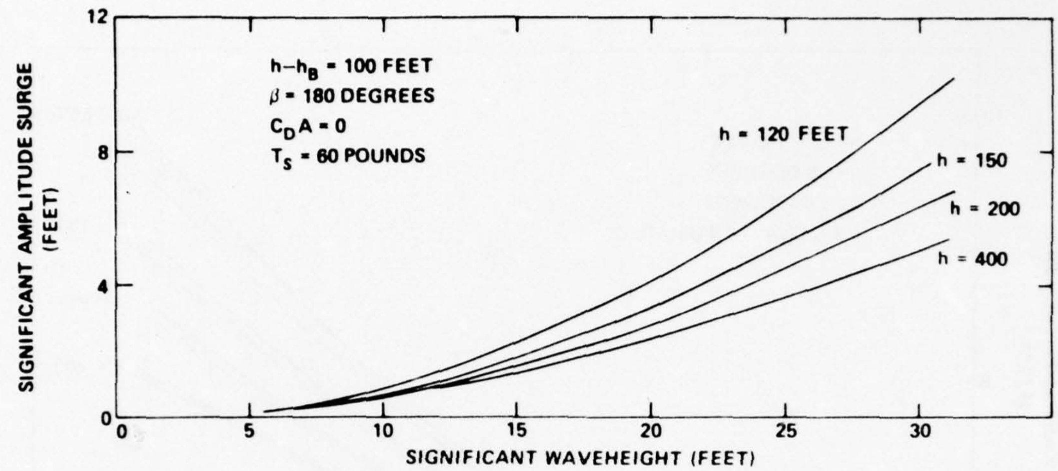

Figure 22 – Effect of Water Depth on Surge Motion in Irregular Waves

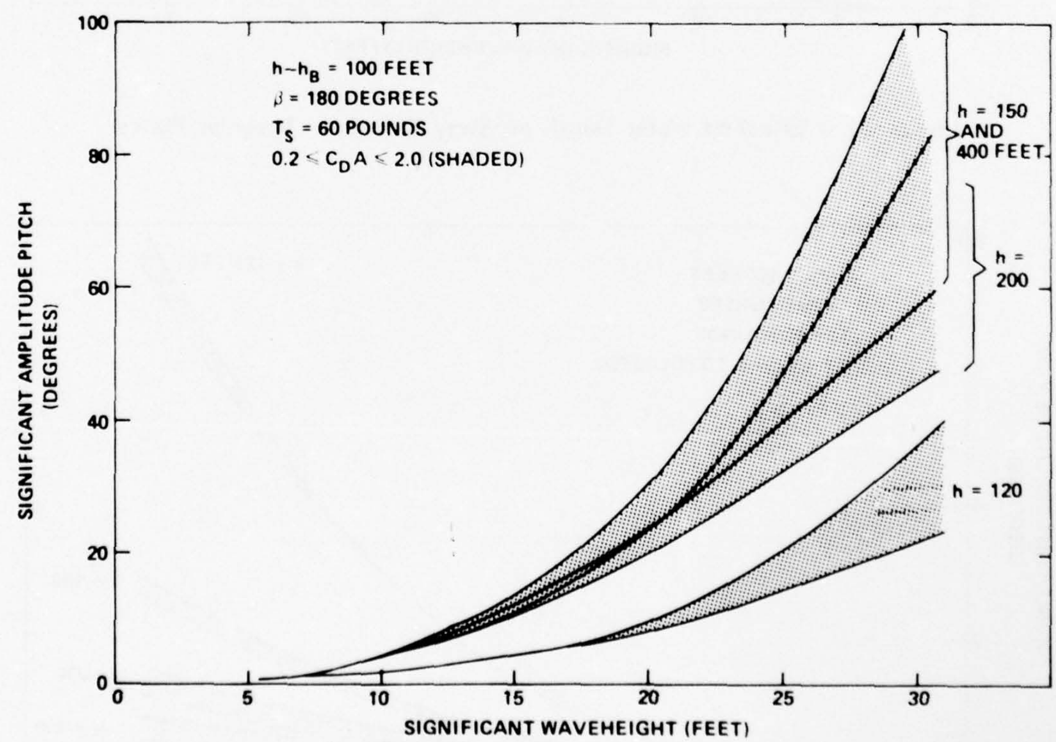

Figure 23 – Effect of Water Depth on Pitch Motion in Irregular Waves

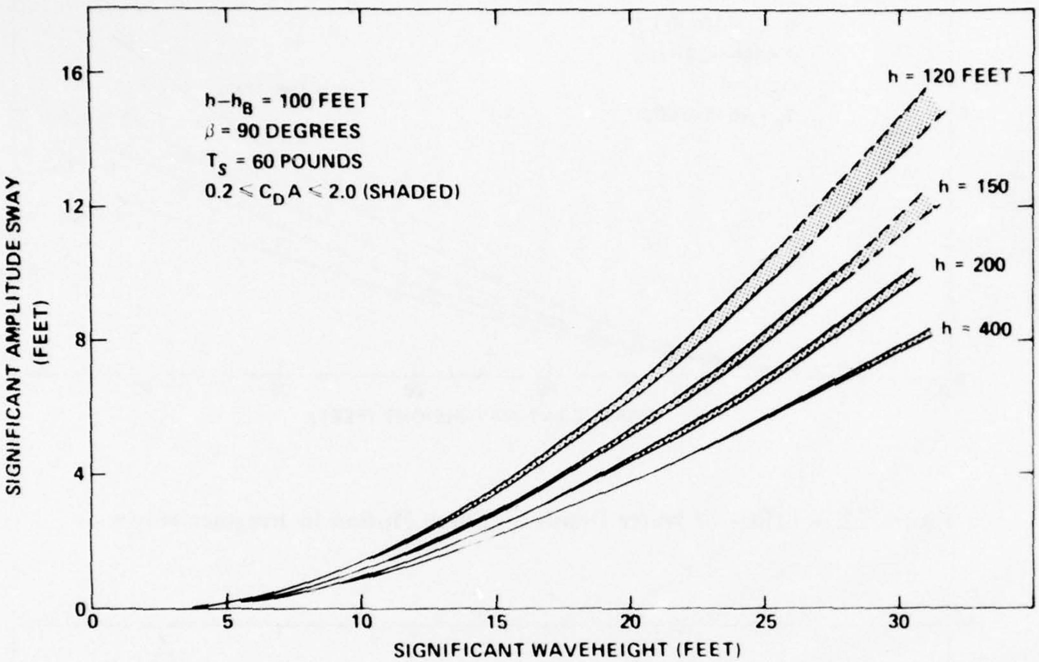

Figure 24 – Effect of Water Depth on Sway Motion in Irregular Waves

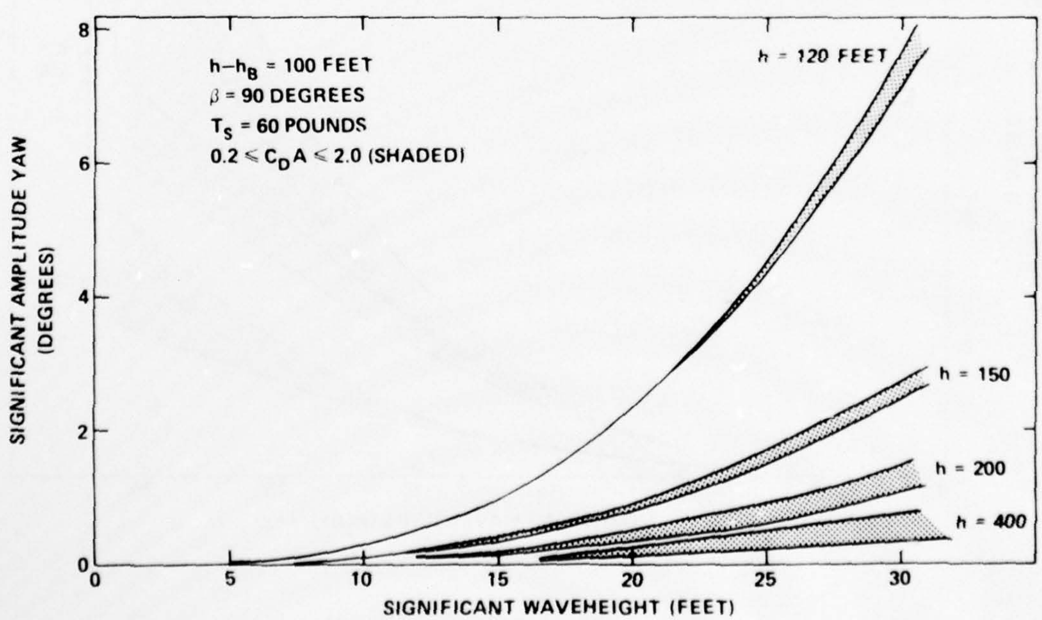

Figure 25 – Effect of Water Depth on Yaw Motion in Irregular Waves

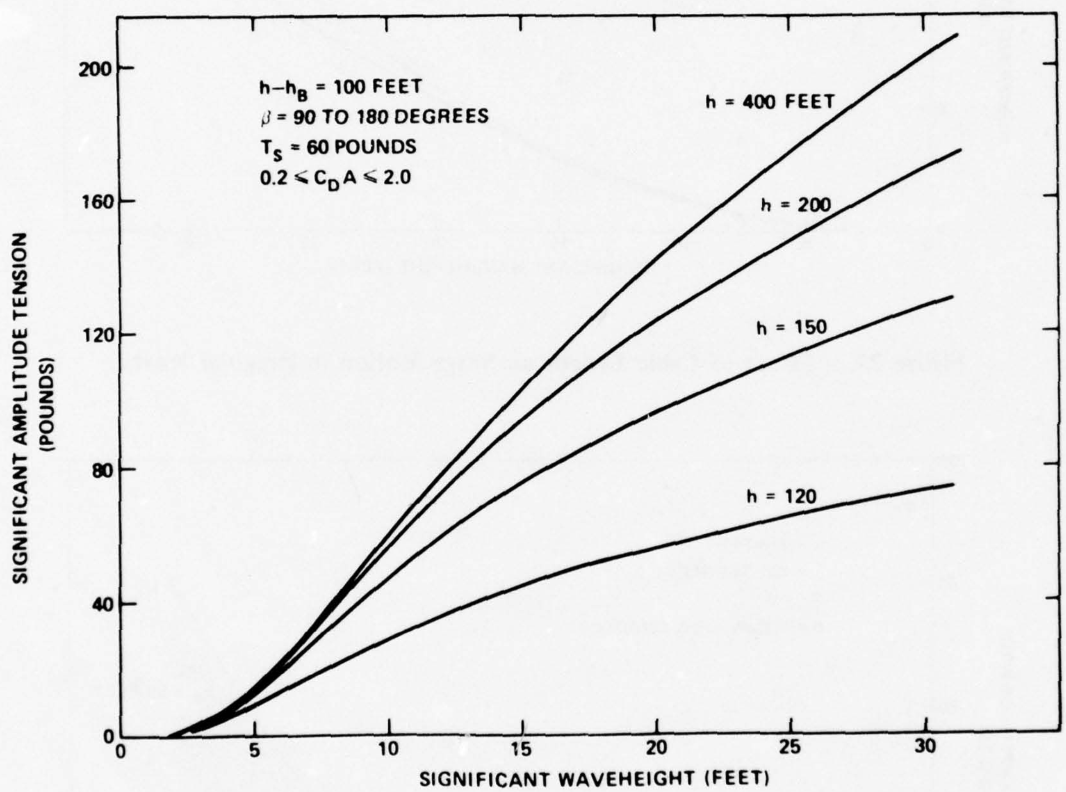

Figure 26 – Effect of Water Depth on Tension in Irregular Seas

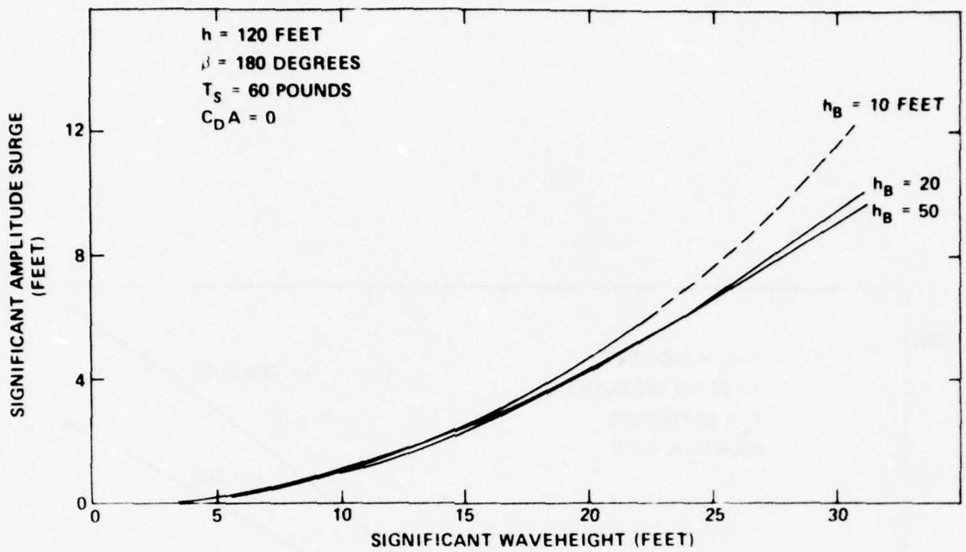

Figure 27 – Effect of Cable Length on Surge Motion in Irregular Waves

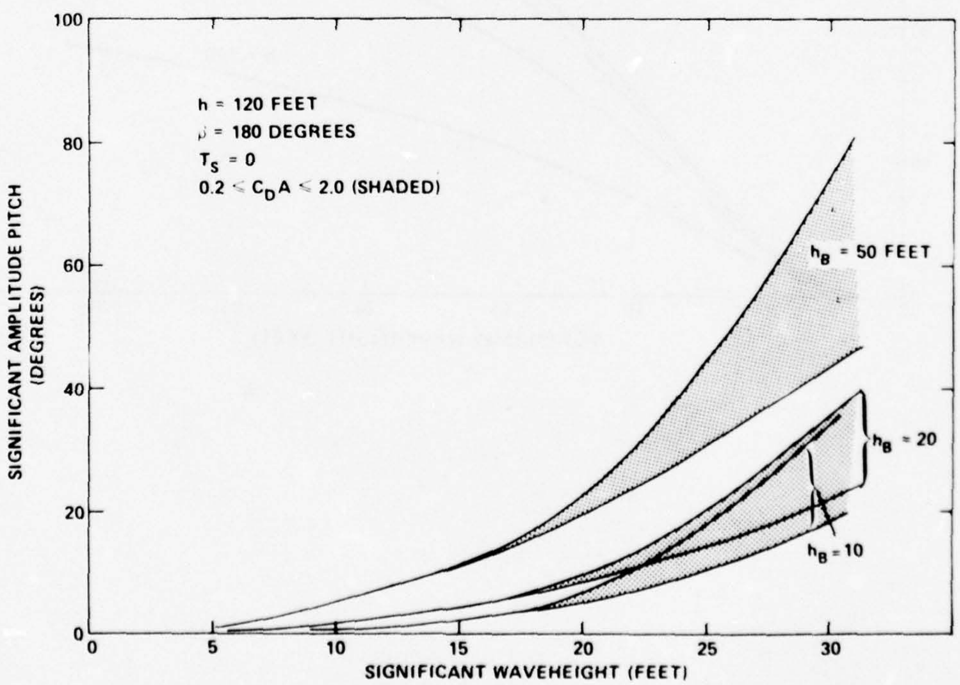

Figure 28 – Effect of Cable Length on Pitch Motion in Irregular Waves

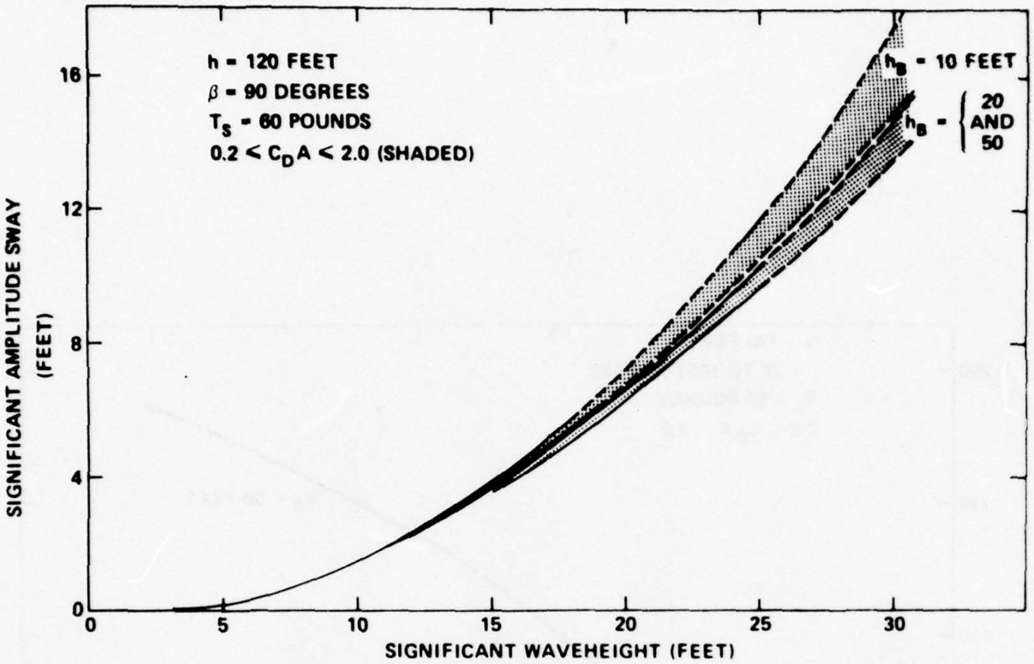

Figure 29 – Effect of Cable Length on Sway Motion in Irregular Waves

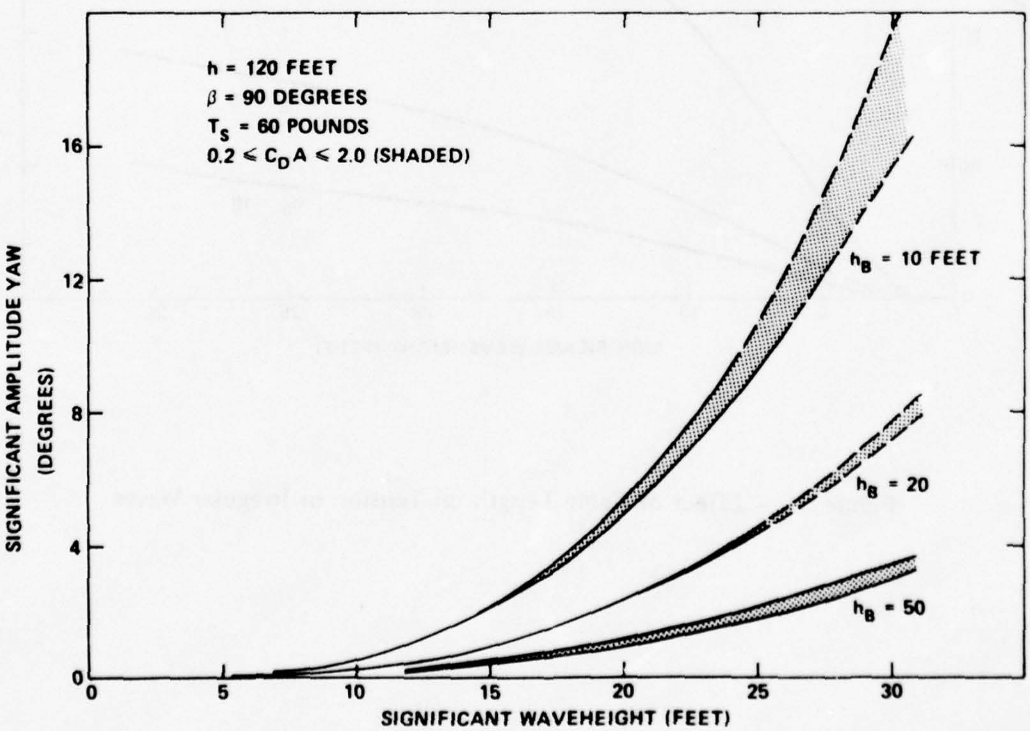

Figure 30 – Effect of Cable Length on Yaw Motion in Irregular Waves

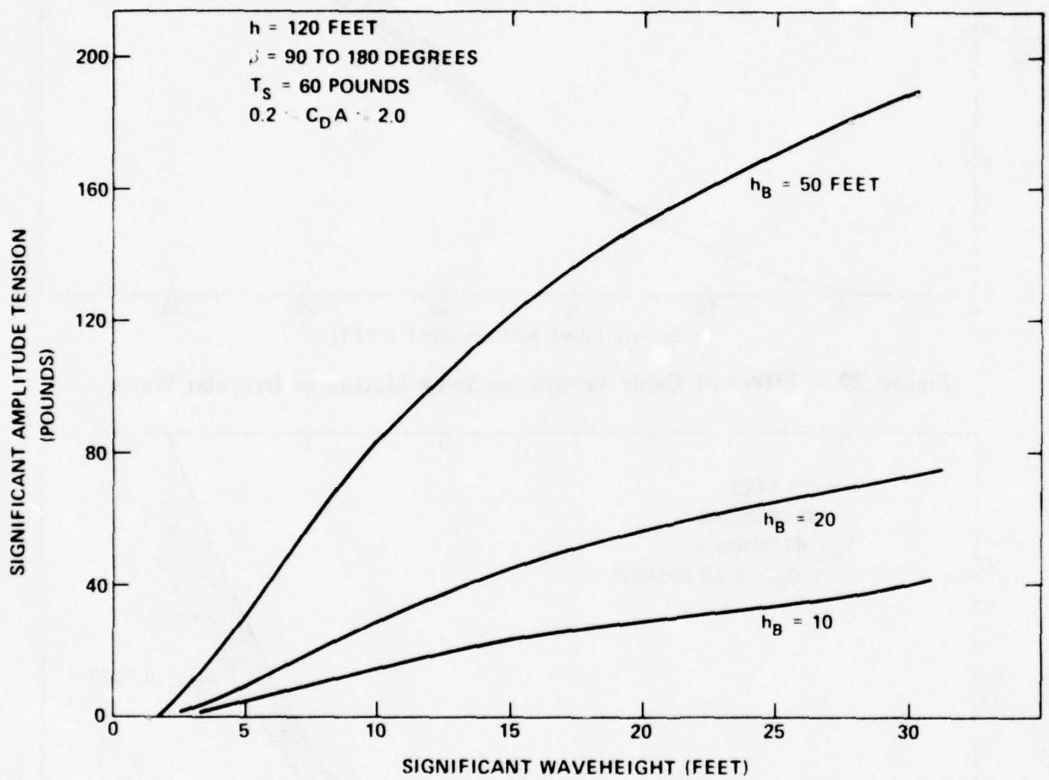

Figure 31 – Effect of Cable Length on Tension in Irregular Waves

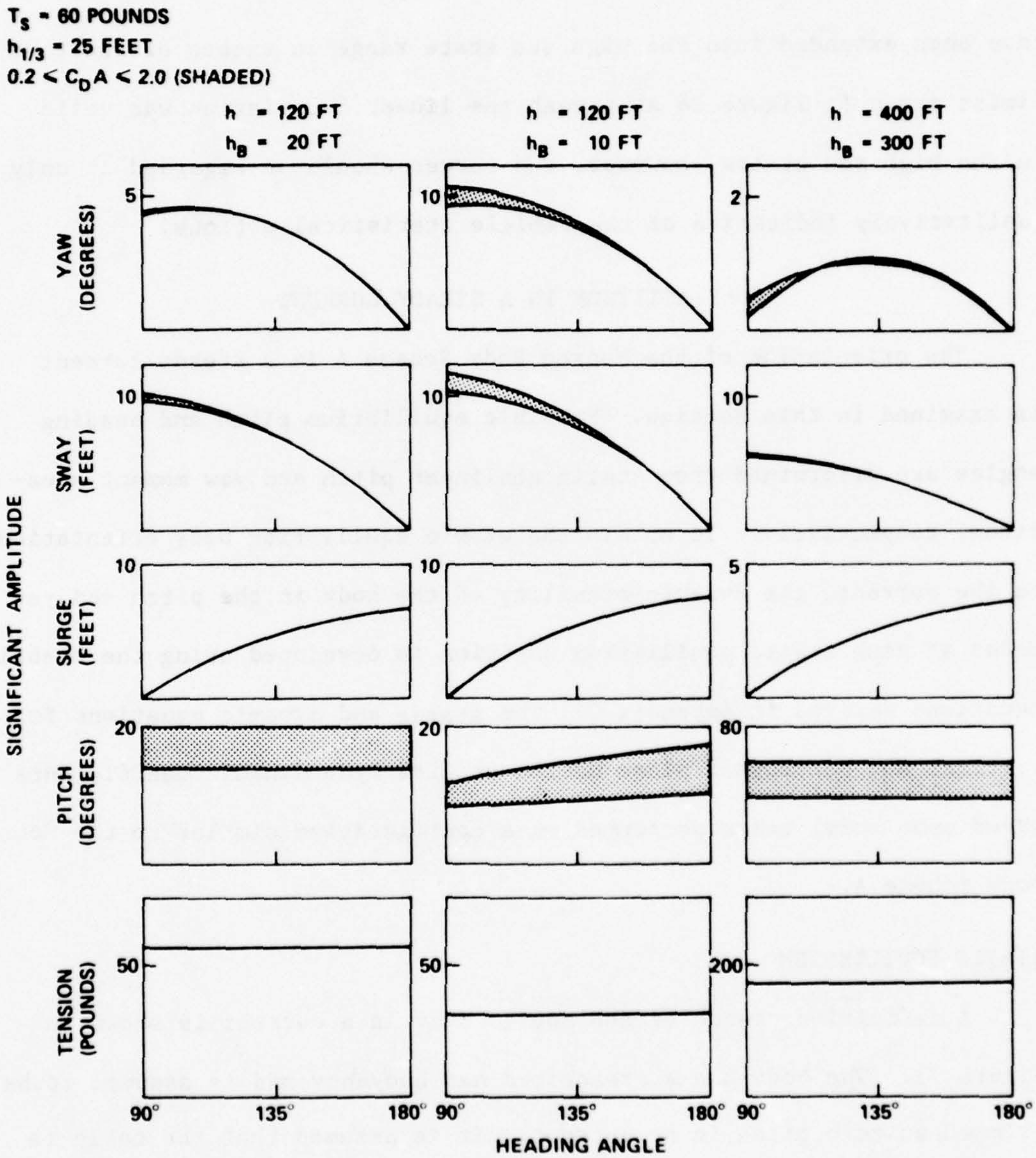

Figure 32 – Effect of Heading Angle on Motion and Tension in Irregular Waves

amplitude of the tension fluctuations can exceed the nominal 60 pound static cable tension at even moderate sea states ($h_{1/3} > 10$ feet for the 400 foot cable length). The motion responses shown in Figures 21-32 have been extended into the high sea state range in excess of the tension limits shown in Figure 26 as though the linear formulation was valid. In the high sea states, however, the curves should be regarded as only qualitatively indicative of the vehicle statistical motions.

BODY ATTITUDE IN A STEADY CURRENT

The orientation of the Moored Body Scheme A in a steady current is examined in this section. Possible equilibrium pitch and heading angles are determined from static nonlinear pitch and yaw moment equations, respectively. To obtain the stable equilibrium body orientations in the current, the dynamic stability of the body in the pitch and yaw modes at each static equilibrium position is developed using the stability equations derived in Appendix C. The static and dynamic equations for vertical and horizontal plane motion utilize hydrodynamic coefficients based upon model tests performed on a configuration similar to the Moored Body Scheme A.

STATIC EQUILIBRIUM

A definition sketch of the moored body in a current is shown in Figure 33. The body has a prescribed net buoyancy and is assumed to be trimmed at zero pitch in no current. It is assumed that the cable is massless and that no hydrodynamic forces act on it. A coordinate system Ox'y'z' is fixed on the body axis at a point directly above the cable attachment point, as shown. Orientation in the vertical and horizontal

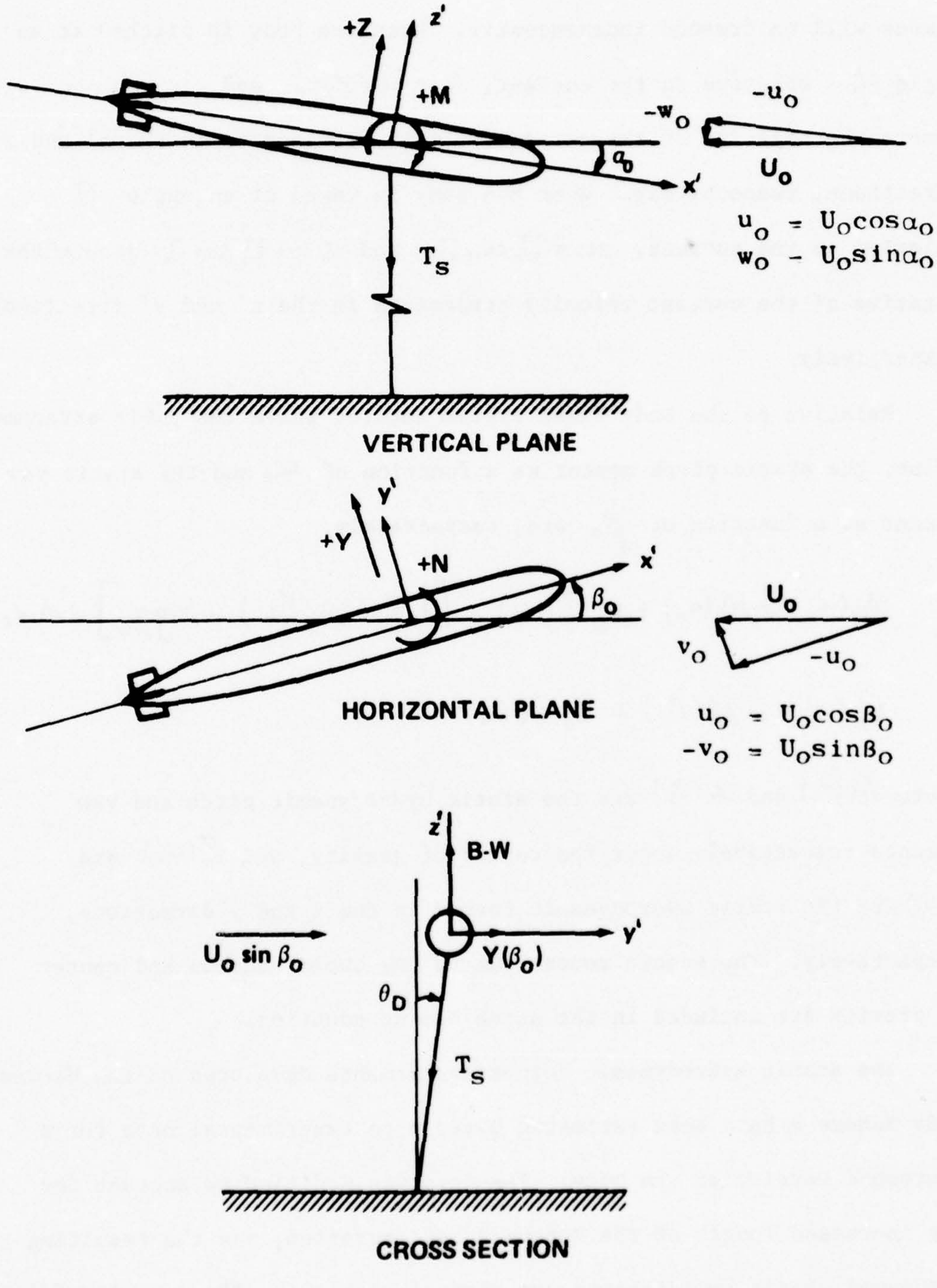

Figure 33 - Definition Sketch of the Moored Body in a Steady Current

planes will be treated independently. When the body is pitched at an angle α_o relative to the current, $u_o = U_o \cos\alpha_o$ and $w_o = U_o \sin\alpha_o$ denote the negative of the current velocity components in the x' and z' directions, respectively. When the body is yawed at an angle β_o relative to the current, $u_o = U_o \cos\beta_o$ and $v_o = -U_o \sin\beta_o$ denote the negative of the current velocity components in the x' and y' directions, respectively.

Relative to the body fixed system located above the cable attachment point, the static pitch moment as a function of α_o and the static yaw moment as a function of β_o are, respectively,

$$M_T(\alpha_o) = M(\alpha_o) + x_G Z(\alpha_o) - \left[T_s R_c\left(1 + \frac{R_c}{h_B}\right) - mg z_G\right] \sin\alpha_o \tag{14a}$$

$$N_T(\beta_o) = N(\beta_o) + x_G Y(\beta_o) \tag{14b}$$

where $M(\alpha_o)$ and $N(\beta_o)$ are the static hydrodynamic pitch and yaw moments respectively about the center of gravity, and $Z(\alpha_o)$ and $Y(\beta_o)$ are the static hydrodynamic forces in the z' and y' directions, respectively. The static moment due to the cable tension and center of gravity are included in the pitch moment equation.

The static hydrodynamic forces and moments developed on the Moored Body Scheme A have been estimated based upon experimental data for a shortened version of the body. The data was modified to account for the increased length of the Scheme A configuration, and the resulting estimated static coefficients are given in Table 4. The notation follows that commonly used in standard submarine equations.[5] The coefficients

---

[5] Gertler, M. and Hagen, G., "Standard Equations of Motion for Submarine Simulation," DTNSRDC Report 2510, June 1967.

Table 4 - Non-Dimensional Static Hydrodymamic Coefficients for the Moored Body Scheme A*

$Z'_w = Y'_v = -0.00676$	$M'_w = -N'_v = 0.00571$
$Z'_{w\|w\|} = Y'_{v\|v\|} = -0.05771$	$M'_{w\|w\|} = -N'_{v\|v\|} = -0.00680$

*Moments referred to the center of gravity. Equilibrium angle of attack is zero.

Table 5 - Non-Dimensional Stability Derivatives for the Moored Body Scheme A*

$Z'_w = Y'_v = -0.01090$	$M'_w = -N'_v = 0.00435$
$Z'_{\dot{w}} = Y'_{\dot{v}} = -0.00899$	$M'_{\dot{w}} = -N'_{\dot{v}} = -0.00081$
$Z'_q = -Y'_r = -0.00377$	$M'_q = N'_r = -0.00181$
$Z'_{\dot{q}} = -Y'_{\dot{r}} = -0.00068$	$M'_{\dot{q}} = N'_{\dot{r}} = -0.00082$
$I'_y = I'_z = I/\frac{\rho}{2}L^5 = 0.00086$	
$m' = m/\frac{\rho}{2}L^3 = 0.01075$	
$x'_G = x_G/L = -0.09948$	

*Moments referred to O_{xyz} system. Equilibrium angle of attack is zero.

are expressed in nondimensional form and are given relative to the body center of gravity. Because of the geometric symmetry of the body, vertical plane coefficients are equally applicable (with appropriate sign changes) for the horizontal plane.

The static hydrodynamic force and moment as a function of angle of attack were originally measured over a $\pm$ 15 degree range. The resulting data were then fitted with a second order polynomial in $\sin\alpha_o$ and $\cos\alpha_o$, the coefficients of which are the static coefficients given in Table 4, and modified for the Scheme A configuration.

The static pitch and yaw moment relative to the point on the body axis directly above the cable attachment as given by Equations (14a) and (14b), respectively, may then be rewritten in nondimensional form in terms of the static coefficients given in Table 4,

$$\frac{M_T(\alpha_o)}{\frac{1}{2}\rho L^3 U_o^2} = \left(M'_w \cos\alpha_o \sin\alpha_o + M'_{w|w|} \sin\alpha_o |\sin\alpha_o| \right)$$
$$+ \frac{x_G}{L}\left(Z'_w \cos\alpha_o \sin\alpha_o + Z'_{w|w|} \sin\alpha_o |\sin\alpha_o| \right)$$
$$- \frac{1}{\frac{1}{2}\rho L^3 U_o^2}\left[T_s R_o (1 + R_o/h_B) - mg z_G \right] \sin\alpha_o \qquad (15a)$$

$$\frac{N_T(\beta_o)}{\frac{1}{2}\rho L^3 U_o^2} = -\left(N'_v \cos\beta_o \sin\beta_o + N'_{v|v|} \sin\beta_o |\sin\beta_o| \right)$$
$$- \frac{x_G}{L}\left(Y'_v \cos\beta_o \sin\beta_o + Y'_{v|v|} \sin\beta_o |\sin\beta_o| \right) \qquad (15b)$$

In Figure 34, the nondimensional static pitch moment given by Equation (15a) is plotted as a function of angle of attack, for several values of the current speed. The hydrodynamic coefficients are given in Table 4, T_s = 60 pounds, $h_B = \infty$, and the vertical center of gravity is located a nominal 0.19 feet below the body axis.

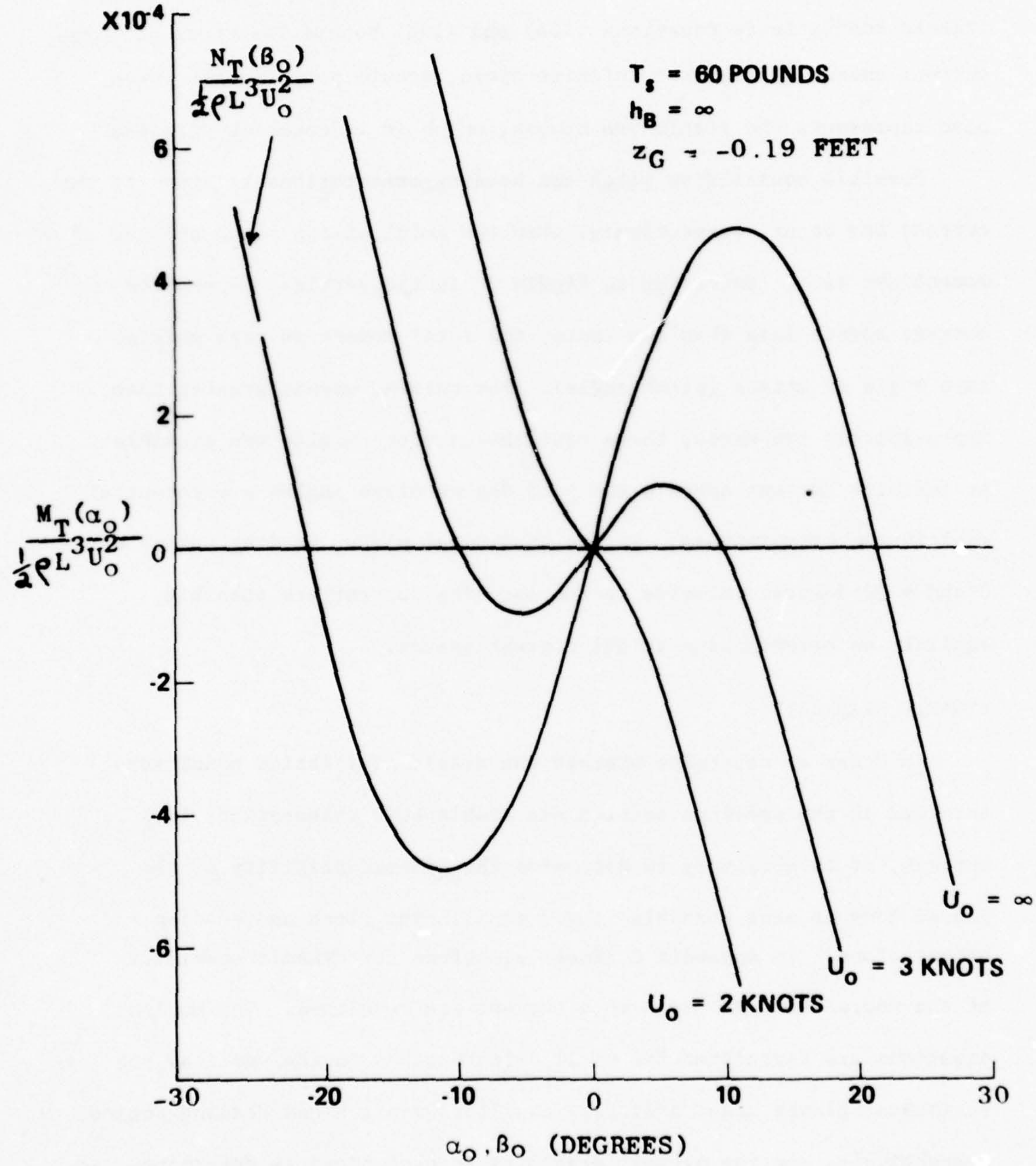

Figure 34 - Static Pitch and Yaw Moment of the Moored Body in a Steady Current

Due to the symmetry of the vertical and horizontal plane hydrodynamic coefficients Equations (15a) and (15b) become identical at large current speed, so that the infinite speed, static pitch moment curve also represents the static yaw moment, which is independent of speed.

Possible equilibrium pitch and heading orientations relative to the current may occur, respectively, when the total static pitch and yaw moment are zero. Referring to Figure 34 in the vertical plane, for current speeds less than two knots, the total moment is zero only at zero angle of attack (pitch angle). For current speeds greater than approximately two knots, three equilibrium pitch angles are possible. At infinite current speed 0 and $\pm$ 23 degree pitch angles are potential equilibrium orientations. In the horizontal plane, heading angles of 0 and $\pm$ 23 degrees relative to the oncoming current are possible equilibrium orientations at all current speeds.

DYNAMIC STABILITY

In order to determine whether the static equilibrium conditions obtained in the previous section are stable body orientations in a current, it is necessary to determine the dynamic stability of the moored body at each possible static equilibrium pitch and heading orientations. In Appendix C linear equations for dynamic stability of the Moored Body Scheme A in a current are developed. The motion equations are formulated for small perturbations in the vertical and horizontal planes about arbitrary equilibrium pitch and heading angles, respectively, and the dynamic stability in each plane is determined from the roots of the governing characteristic equation.

The hydrodynamic force and moment coefficients used in the determination of the stability criteria are the stability derivatives, which represent the slopes of the force or moment with respect to a given

motion variable at a prescribed angle of attack α_0 (or drift angle β_0).

The stability derivatives at zero angle of attack for a configuration of the Moored Body which is shorter in length are available from a previously conducted program of experirents.

These coefficients were modified to account for the increased length of the Scheme A configuration, and then adjusted for the fact that the origin of the body fixed coordinate system was located directly above the cable attachment point. These derivatives are provided in Table 5. Since the derivatives are taken about zero angle of attack, a quantitative description of the dynamic stability is possible only at $\alpha_0 = 0$ and $\beta_0 = 0$. However, based upon estimated values for the derivatives at other angles, some qualitative predictions can be made regarding the dynamic stability at equilibrium pitch and heading angles other than zero.

Vertical Plane

In Appendix C the basic equations for coupled surge and pitch motion of the moored body in a current are given by Equations (C3) and (C4). This system of equations results in a fourth order characteristic equation, the roots of which determine the nature of the coupled surge and pitch motion.

A simpler condition for vertical plane stability is obtained from the equation for uncoupled pitch motion. A condition for dynamic stability in the pitch mode which neglects the effect of surge coupling but includes (non-rigorously) the restoring moment due to the vertical center of gravity is given by Equation (C7) of Appendix C,

$$\frac{\rho}{2} L^3 U_0^2 M'_w \leq (T_0 R_0 - m g z_G) \cos \alpha_0 \tag{16}$$

For an equilibrium pitch angle of zero ($\alpha_o = 0$), with $T_s = 60$ pounds, $z_G = -0.19$ feet, and M_w' given from Table 5 vertical plane stability is obtained when $U_o < 2.4$ knots.

Figure 34 indicates that for current speeds roughly greater than two to three knots, a static equilibrium occurs at angles of attack other than zero; specifically $\pm$ 23 degrees at infinite current speeds. The stability derivative M_w' is only available at $\alpha_o = 0$, its value at other equilibrium angles may be qualitatively estimated from Figure 34, however. The slope at $\alpha_o = 0$ of the nondimensional total moment curve for infinite current speed given in Figure 34 represents the stability derivative M_w'. At $\alpha_o = 0$ this slope is equal to the value of M_w' given in Table 5, and is a positive quantity. For static angles of attack greater than approximately 10 degrees, the slope of the infinite speed total moment curve becomes negative, therefore M_w' is negative and from Equation (16) dynamic stability is obtained whenever M_w' is negative.

The vertical plane stability characteristics for the Moored Body Scheme A with $T_s = 60$ pounds, $z_G = -0.19$ feet and $h_B = \infty$ may be summarized as follows

(a) For $U_o < 2.4$ knots the body is dynamically stable at zero equilibrium pitch angle.

(b) For $U_o > 2.4$ knots the body becomes dynamically unstable at zero pitch angle but becomes dynamically stable at plus and minus equilibrium pitch angles which deviate from zero angle with increasing current speed. At infinite current speed the body is stable at $\pm$ 23 degree pitch angles.

Horizontal Plane

From Figure 34 the static yaw moment acting on the moored body is given by the curve for infinite speed which is zero at heading angles of $\pm$ 23 degrees and zero degrees relative to the oncoming current. In order to determine the orientation the body actually assumes, it is necessary to determine the dynamic stability at these possible equilibrium headings.

The expressions for coupled sway and yaw motion of the moored body in a current are given by Equations (C-10) and (C-11) of Appendix C. This system of equations results in a cubic characteristics equation (Equation C-12) the roots of which determine the nature of the coupled sway and yaw motion. Using the horizontal plane stability derivatives for zero drift angle ($\beta_o = 0$) as given in Table 5, Equation (C-12) becomes

$$\sigma'^3 + 1.80\,\sigma'^2 + \left(-0.73 + \frac{56.30\,T_s}{\frac{1}{2} L h_B U_o^2}\right)\sigma' + \frac{34.60\,T_s}{\frac{1}{2} L h_B U_o^2} = 0 \tag{17}$$

where $\sigma' = \frac{L}{U_o} s$ is the nondimensional root, and $s = d/dt$.

For a nominal static cable tension of 60 pounds and minimum cable length of 20 feet, the stability requirements given by Equation (C-13) of Appendix C are satisfied when the current speed $U_o < 1.75$ knots. When the cable length is increased to 50 feet, the body is dynamically stable at $\beta_o = 0$ for $U_o < 1.10$ knots. For infinite cable length Equation (17) reduces to a quadratic, the third term of which is negative, thus indicating the body to be unstable at all current speeds.

Specific values for the stability derivatives are not available for the $\pm$ 23 degree equilibrium headings. However, the critical derivative affecting the stability characteristics is N_v' and this coefficient may be estimated, as in the case of vertical plane stability, from the slope

of the infinite speed moment curve of Figure 34. From Figure 34 it is noted that the slope of the total moment at $\beta_o = \pm 23$ degrees is of opposite sign to the slope at $\beta_o = 0$. Substitution of a large positive value for N_v' into Equation (C-12) means that the third term of Equation (17) becomes positive for all combinations of cable tension and length and current speed. Anticipated changes in the other stability derivatives at $\beta_o = 23$ degrees are not expected to significantly alter the characteristic equation. With all of the terms in Equation (17) of the same sign and Equation (C-13) satisfied, the moored boy is stable at $\beta_o = \pm 23$ degrees for all conditions.

The horizontal plane stability characteristics of the Moored Body Scheme A may be summarized as follows:

(a) The body is dynamically stable at heading angles of $\pm$ 23 degrees relative to the oncoming current for all current speed, tension, and cable length conditions.

(b) The body is also dynamically stable at a zero degree heading for current speeds less than 1.75 knots when the cable length is minimum (20 feet). As the cable length increases the stable speed range at zero heading is reduced until the body is dynamically unstable at infinite cable length for all current speeds.

(c) Although the moored body with finite cable length is stable at low current speeds at zero heading angle, stability at the $\pm$ 23 degree headings is stronger, and it is expected the body would assume these heading orientations subject to large perturbations.

CABLE ORIENTATION

An analysis of the dynamic stability of the Moored Body Scheme A in a current indicates that for low current speeds the body assumes a zero pitch attitude and possible ± 23 degrees heading angles relative to the oncoming current. With this given orientation of the body relative to the current, the static cable deflection angle and cable tension may be determined.

The total lateral force as a function of static heading (drift) angle is given by

$$Y(\beta_o) = \frac{\rho}{2} L^2 U_o^2 \left(-Y'_v \cos\beta_o \sin\beta_o - Y'_{v|v|} \sin\beta_o |\sin\beta_o| \right)$$

where the coefficients are given in Table 4.

A force balance, as shown in Figure 33, provides expressions for the static cable deflection and static cable tension.

$$\theta_D = \tan^{-1} \frac{Y(\beta_o)}{B-W} \qquad T_s = \left[(B-W)^2 + Y(\beta_o)^2 \right]^{1/2}$$

With β_o = 23 degrees, Figures 35 and 36 show the static cable deflection and tension, respectively, for several values of the buoyancy minus weight. For current speeds, less than about one knot, the cable deflection is less than 20 degrees and static tension is virtually the same as the net buoyancy.

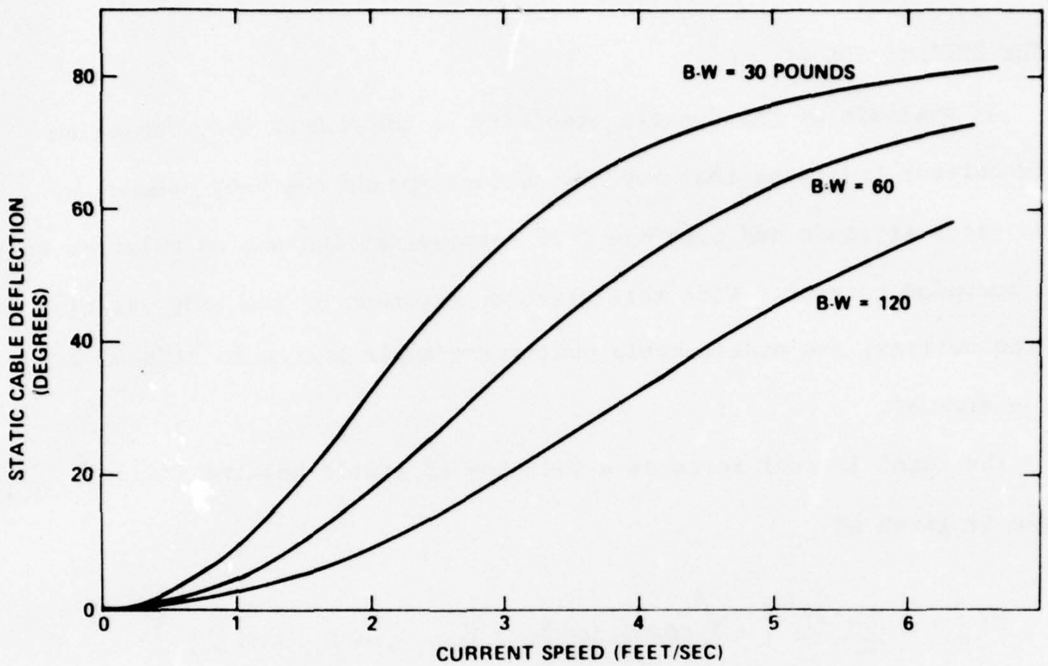

Figure 35 – Static Cable Deflection in a Steady Current

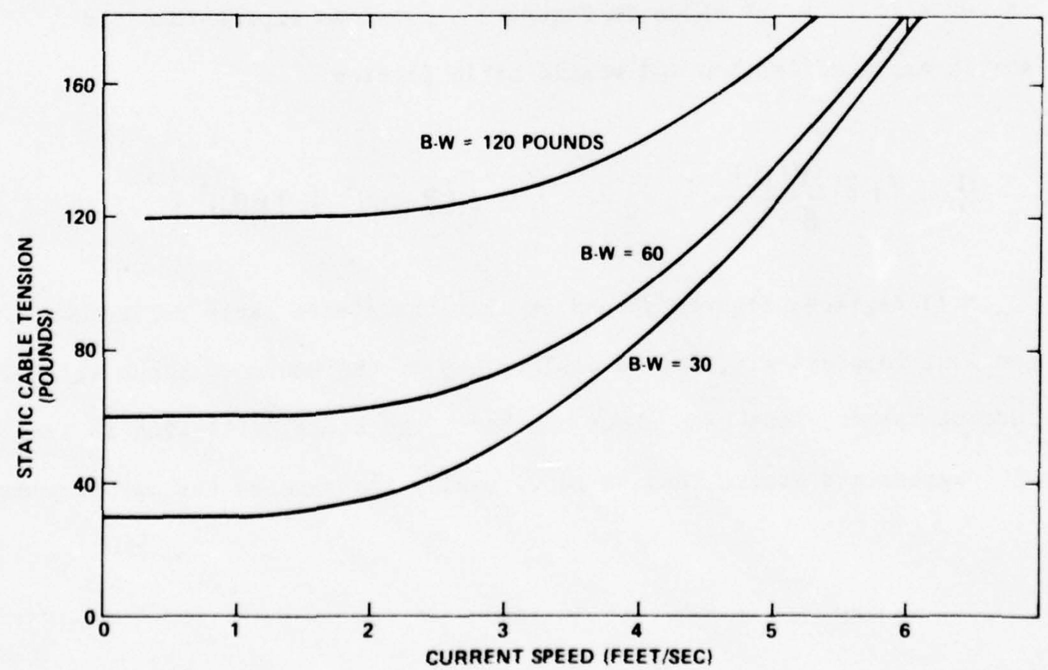

Figure 36 – Static Cable Tension in a Steady Current

WAVE-CURRENT INTERACTIONS

In the first part of this report, the oscillatory motions of the Moored Body Scheme A in response to exciting waves were determined in the absence of a current. In the second section the stability and orientation of the body in a steady current in the absence of wave excitations have been determined. Clearly, these two cases must represent the extremes when the simultaneous effect of current and waves are present. We now examine the behavior of the body when it is subject to waves and a steady current.

In order to quantitatively determine the interaction of waves and current, when current speed and oscillatory velocities are of the same order, a formulation of the equations of motion accurate to second order is necessary. This is beyond the scope of the present analysis. However, a brief, and by no means rigorous, examination of certain second order effects has provided some qualitative predictions of the wave-current coupling.

Briefly, the second order equations in the yaw plane were formulated. The form is essentially that of Equations (C8) and (C9) in Appendix C except that the nonlinear force and moment, $Y_{v|v|}v|v|$ and $N_{v|v|}v|v|$ are included, and where the lateral velocity v appears, the relative velocity ($U_0 \sin\beta_0 - \dot{\xi}_2$) would be substituted. Also, the wave exciting forces appear on the right-hand side of the equation. Steady second order forces and moments, due to the wave excitation, have been neglected since the body is submerged at least 100 feet below the surface.

By taking the Fourier components of each term in the second order

equations, separate equations for the steady forces and the first order harmonic forces are obtained. Solution of the steady equations provides the mean orientation, and solution of the first harmonic equation provides the oscillatory motions. Results of this analysis indicate that:

(a) The steady yaw moment equation reduces to Equation (15b) when oscillation motions are zero, and the first harmonic equations reduce to Equations (7) and (8) when current speed is zero.

(b) The combination of steady current and oscillatory body motion in the cross-flow drag terms provides an additional steady force and moment which tends to orient the body into the current. When current speed is much larger than oscillatory velocities, this steady force is proportional to the square of body motion amplitude. When the oscillatory velocity is much larger than current speed, the steady force is proportional to the product of current speed and oscillatory motion amplitude.

(c) The forces and moments due to lift $Y_v V$ and $N'_v V$, respectively, provide linear damping in the first harmonic equations proportional to the product of current speed and oscillatory velocity. This is the predominant damping term when the current speed is large compared to oscillatory velocities. When oscillatory velocities are large, the nonlinear damping proportional to the oscillation velocity squared is predominant.

Based upon results of the second order analysis, the behavior of the Moored Body Scheme A in response to various combinations of waves and current may be summarized as follows:

1. When the vehicle is subject to a current with no wave excitation,

stable heading angles of $\pm$ 23 degrees relative to the current direction are usually attained, although under certain conditions of current speed, cable length and tension, a zero degree heading can also be achieved. When the current speed is less than about 2.4 knots, the vehicle is stable at a zero degree pitch angle.

2. When very small wave excitations are superimposed on the current, the body assumes mean displacement, heading, and pitch angles determined by the steady current. The oscillatory motions may be regarded as small perturbations about the equilibrium position. The equations governing oscillatory motion contain linear damping, the coefficient of which is directly proportional to the current speed.

3. As oscillatory velocity increases, but remains less than current speed, steady forces and moments, resulting from the nonlinear drag, tend to reduce the stable heading angles relative to the current direction. Both the linear damping due to lift and the nonlinear damping due to cross-flow drag appear in the equations for oscillatory motion.

4. When current speed is of the same order or greater than oscillatory velocities, the vehicle assumes a heading angle into the current, and the nonlinear drag is the predominant damping effect in the equations of oscillatory motion. The oscillatory equations are approximated by Equations (5) through (8).

5. When the body is excited by waves with no current, there are no steady forces generated and the vehicle assumes no preferred direction.

When the body is simultaneously subject to current and waves, depending upon current speed, wave amplitude, and the angle between current and wave propagation direction, the vehicle may assume any one of the above conditions. However, for specified current speeds less than 1 knot, condition 4 is probably the most likely situation. From the oscillatory motion results of the first section, the motion velocities $\dot{\xi}_1$, $\dot{\xi}_2$, $L/2\,\dot{\xi}_5$ and $L/2\,\dot{\xi}_6$ are at least of order ωA. With constant wave slope of $A/\lambda \simeq \frac{1}{100}$, $\omega A > 1$ knot and $\dot{\xi}_1$, $\dot{\xi}_2$, $\frac{L}{2}\dot{\xi}_5$, and $\frac{L}{2}\dot{\xi}_6 > U_0$.

In summary, when the body is simultaneously subject to waves and a small current, the oscillatory motions are represented by the zero current condition. The only effect of current then is to orient the body so that the mean heading and pitch angles are directed into the current.

CONCLUSIONS

Based upon the results attained from a theoretical investigation of the motions of the Moored Body Scheme A in waves and current, the following conclusions are drawn:

1. In the absence of any wave disturbance, the body is dynamically stable at a zero-degree pitch angle for current speeds less than 2.4 knots. For current speeds greater than 2.4 knots the stable pitch angle shifts away from zero and approaches $\pm$ 23 degrees as the current speed becomes extremely large. The vehicle is stable at $\pm$ 23 degrees heading angles relative to the incident current at all current speeds, and a stable zero degree heading angle may also be achieved for limited combinations of current

speed, cable length and static cable tension. For specified current speeds less than 1 knot, the static cable deflection from the vertical is less than 10 degrees, and the static cable tension is not signficantly changed from the prescribed net buoyancy of 60 pounds.

2. When wave induced oscillatory velocities are small compared to current speed, oscillatory motions take place about a mean orientation defined by the steady current.

3. For current speeds less than 1 knot, oscillation velocities are typically greater than the current speed. In this case oscillatory motions are approximated by the zero current formulation, the only effect of wave coupling being to align the vehicle so that the mean pitch and yaw angles are into the current.

4. The zero current formulation of wave induced oscillatory motions indicates that the mooring system introduces resonances in all of the modes of motion. Pitch motion, however, is the only mode where the resonant frequency is high enough to be grossly excited in a real seaway. The pitch resonance occurs at approximately 0.33 radians/sec. Due to the nonlinear character of the damping forces, a precise prediction of the motion near resonance is not possible. However, an envelope for the motion defined by reasonable limits of the damping coefficient indicates pitch motion amplitudes in excess of 30 degrees in sea states 6 and 7.

5. A minimum submergence depth of 100 feet and infinite water depth provide a worst case for pitch motion and cable tension fluctuations. The 100-foot depth of submergence and minimum 120-foot water

depth provide a worst case for horizontal plane motions. An increase in static cable tension tends to increase all motion quantities by shifting resonances to higher frequencies.

6. For a nominal static cable tension of 60 pounds, the significant amplitudes of the motions and tension for the worst case conditions are:

Sea State ≤ 5 ($h_{1/3} < 13$ feet)

Surge and sway do not exceed two feet. Pitch and yaw angles do not exceed 10 and 1 degrees, respectively. Cable tension fluctuations can exceed static cable tension.

Sea States 6 and 7

The cable tension fluctuations exceed the static cable tension (the significant amplitude of T_3 is about 170 pounds at $h_{1/3}$ = 25 feet) and the body can experience motion in the heave mode. The linear formulation of the equations of motion are no longer strictly valid in this range. Qualitatively all motion increases rapidly with increasing sea state, and the pitch motion may be in excess of 30 degrees at $h_{1/3}$ = 20 feet.

ACKNOWLEDGMENTS

The author wishes to thank Dr. J. P. Feldman for his guidance throughout the course of this investigation and for his careful review of this report.

The author also wishes to acknowledge the work of Dr. C. M. Lee who initially developed the expressions for the wave forces on a body of revolution in finite depth water and who suggested the method used herein to incorporate the non-linear viscous damping in the equations of motion.

APPENDIX A
WAVE EXCITING FORCES

APPENDIX A

WAVE EXCITING FORCES

In the main body of this report the linear equations of motion in five degrees of freedom are developed for a slender body of revolution tehered near a horizontal bottom and subject to the forces induced by incident plane surface waves. On the right-hand side of the motion equations appear the complex amplitudes of the wave exciting forces, F_{oi}, where $i = 1,2,3,5,6$ correspond to the surge sway, heave, pitch and yaw modes, respectively.

In this section expressions for the first order wave exciting forces, which include body diffraction and bottom effects, are developed from finite depth, two-dimensional, potential flow theory. Three-dimensional forces are obtained in a stripwise sense by integrating transverse sectional forces over the length of the body.

We assume that the fluid is inviscid, incompressible, and irrotational, the incident waves are linear and the wavelength large compared to the transverse dimensions of the body ($2\pi R_o/\lambda << 1$), and the body is deeply submerged such that it behaves as a weak scatterer of the incident waves.*

If p denotes the pressure on the body surface, S_o, the force and moment acting on the body can be expressed by[1]

$$\vec{F} = \iint_{S_o} p\vec{n}\, ds \quad \text{(A1-a)} \qquad \vec{M} = \iint_{S_o} p(\vec{r}_o \times \vec{n})\, ds \quad \text{(A1-b)}$$

---

* This means that the disturbance created by wave diffraction does not alter the free surface.

where $\vec{n}$ is a unit normal vector on and positive into the body surface, and $\vec{r}_o$ is a vector from the origin of the coordinate system to a point on the body surface.

Since the fluid is assumed irrotational, a velocity potential, $\Phi(x, y, z, t)$, the gradient of which represents the velocity field in the fluid, can be introduced. The pressure in the fluid is then related to the velocity potential by Bernoulli's Equation for unsteady flow, which is given as

$$p = -\rho \frac{\partial \Phi}{\partial t} \tag{A2}$$

where the static head and velocity squared terms have been neglected.

For a body in waves and restrained from motion, the velocity potential consists of two parts; one representing the disturbance generated by the undisturbed incident wave, Φ_I, and the other due to the scattering or diffraction of the incident wave from the body, Φ_D.

$$\Phi = \Phi_I + \Phi_D \tag{A3}$$

The velocity potential for plane, progressive, linear waves propagating in a finite depth fluid can be expressed by[1]

$$\Phi_I = \text{Real}\left\{ \frac{gA}{\omega} \frac{\cosh k(z+h)}{\cosh kh} \exp\left[ikx\cos\beta + iky\sin\beta - i\omega t\right]\right\} \tag{A4}$$

where the relationship between the wavelength and frequency is given by Equation (3) in the main text.

On the rigid body surface the normal velocity component of the fluid must be zero.

$$\vec{\nabla}\Phi\cdot\vec{n} = \frac{\partial\Phi}{\partial n} = (\Phi_{In} + \Phi_{Dn}) = 0 \quad on\ S_o$$

thus on S_o $\quad \Phi_{Dn} = -\Phi_{In}$ $\quad$ and

$$\frac{\partial\Phi_D}{\partial n} = -\frac{KgA}{\omega}\frac{\cosh K(z+h_c)}{\cosh Kh}\exp[iKx\cos\beta + iKy\sin\beta - i\omega t]$$

$$\times\{in_1\cos\beta + in_2\sin\beta + n_3\tanh K(z+h_c)\}$$

where n_1, n_2, and n_3 are the components of $\vec{n}$ along the x , y , and z directions, respectively. Since $n_1 \ll n_2$ or n_3 for a slender body except near the body ends, we can neglect the contribution of n_1 in the above expression and obtain

$$\Phi_{Dn}\Big|_{S_o} = -\frac{KgA}{\omega}\frac{\cosh K(z+h_c)}{\cosh Kh}\exp[iKx\cos\beta + iKy\sin\beta - i\omega t]$$

$$\times\{in_2\sin\beta + n_3\tanh K(z+h_c)\} \qquad \text{(A5)}$$

Formally, Φ_D is obtained by the solution of a boundary value problem, where in addition to the usual free surface, radiation, and bottom conditions, Φ_D must also satisfy Equation (A5) on the body surface, S_o. Lee and Newman[6] have shown for the infinite depth case that an approximate expression for Φ_D can be obtained in terms of the two-dimensional potentials

for forced harmonic motion, $\phi_2(y,z)$ and $\phi_3(y,z)$, where

$$\frac{\partial \varphi_2}{\partial n} = n_2 \quad \text{and} \quad \frac{\partial \varphi_3}{\partial n} = n_3 \qquad \text{on } S_o$$

Applying this same approach to the finite depth case, Φ_D can be given to leading order in Ky and Kz by

$$\Phi_D = -\frac{KgA}{\omega}\left[i\varphi_2 \gamma \sin\beta + \varphi_3 \delta \right] \times \exp\left[ikx\cos\beta - i\omega t \right] \tag{A6}$$

where

$$\gamma = \frac{\cosh Kh_c}{\cosh Kh} \quad \text{and} \quad \delta = \frac{\sinh Kh_c}{\cosh Kh}$$

The velocity potentials, $\phi_2(y,z)$ and $\phi_3(y,z)$, correspond to the two-dimensional flow disturbances generated by the forced oscillation of the body in the horizontal and vertical directions, respectively. When the body is deeply submerged such that the generated disturbances do not disturb the free surface, Lee and Newman[6] showed that ϕ_2 and ϕ_3 can be expressed in the form

$$\varphi_2(r,\theta;x) = -\frac{\cos\theta}{2\pi r}\left[S_A(x) + a_{22}(x)/\rho \right] \tag{A7}$$

$$\varphi_3(r,\theta;x) = -\frac{\sin\theta}{2\pi r}\left[S_A(x) + a_{33}(x)/\rho \right] \tag{A8}$$

---

[6] Lee, C.M., and J.N. Newman, "The Vertical Mean Force and Moment of Submerged Bodies Under Waves," Journal of Ship Research, Vol. 15, No. 3, September 1971.

where $S_A(x)$ is the sectional area and $a_{22}(x)$ and $a_{33}(x)$ are the sectional added masses for motion in the sway and heave directions, respectively.

The added masses for a circular cylinder translating in the transverse directions near a rigid wall, is[7]

$$a_{22} = a_{33} = \rho S_A(x)\left[1 + \frac{R(x)^2}{2h_c^2}\right] \qquad R/h_c \ll 1 \tag{A9}$$

Using the expressions for a_{22}, a_{33}, ϕ_2 and ϕ_3, an approximate expression for ϕ_D is given by

$$\Phi_D = -\frac{kgA}{\omega}\, e^{-i\omega t + ikx\cos\beta}\, \frac{S_A(x)}{2\pi} \tag{A10}$$

$$\left[\left(2 + \frac{S_A(x)}{2\pi h_c^2}\right)\left(-i\gamma\sin\beta\,\frac{\cos\theta}{r} - \frac{\delta\sin\theta}{r}\right)\right]$$

When the body is a slender body of revolution, the surface integral can be written in terms of the cylindrical coordinates as

$$\iint_{S_0} \cdots\, ds = \int_L dx \int_0^{2\pi} \cdots\, R(x)\, dx \tag{A11}$$

The normal vector can also be written

$$\vec{n} = (n_1, n_2, n_3) = \left(\frac{d}{dx}R(x),\ -\cos\theta,\ -\sin\theta\right) \tag{A12-a}$$

and

$$\vec{r}_c \times \vec{n} = (n_4, n_5, n_6) = (0,\ -x n_3,\ x n_2) \tag{A12-b}$$

[7] Kennard, E. H., "Irrotational Flow of Frictionless Fluids, Mostly of Invariable Density," NSPDC Report 2299, 1967.

Substitution of Equations (A2), (A3), and (A11) into Equations (A1-a) and (A1-b) provide the components of the wave exciting force and moment as follows:

$$F_i = -\rho \int_L dx\, R(x) \int_0^{2\pi} d\theta\, n_i \frac{\partial}{\partial t} \left(\Phi_I + \Phi_D \right) \tag{A13}$$

where i = 1, 2, and 3 denotes forces in the x, y, and z directions and i = 5 and 6 denotes the pitch and yaw moments, respectively.

The expressions for Φ_I and Φ_D given by Equations (A4) and (A10), respectively, and the surface normal components given by Equations (A12-a) and (A12-b) may then be substituted in Equation (A13). With $y = r \cos \theta$ and $z = r \sin \theta$, the integrand can be expanded in powers of KR(x) on the body surface, and the integration around the circular cross-section of leading order terms may be accomplished explicitely. Resulting expressions then involve lengthwise integrations which may be computed once the radius is specified along the length of the body. The expressions for the wave exciting forces and moments in five degrees of freedom are:

$$F_1 = \rho g K A \gamma \cos\beta\, e^{-i\omega t} \left\{ \int_L dx\, S_A(x)\, e^{iKx\cos\beta} \right\} \tag{A14-a}$$

$$F_2 = \rho g K A \gamma \sin\beta\, e^{-i\omega t} \left\{ \int_L dx\, S_A(x) \left[2 + \frac{R(x)^2}{4h_c^2} \right] e^{iKx\cos\beta} \right\} \tag{A14-b}$$

$$F_3 = \rho g K A \delta\, e^{-i\omega t} \left\{ -i \int_L dx\, S_A(x) \left[2 + \frac{R(x)^2}{4h_c^2} \right] e^{iKx\cos\beta} \right\} \tag{A14-c}$$

$$F_5 = \rho g K A \delta e^{-i\omega t}\left\{ i \int_L dx\, S_A(x)\, x \left[2 + \frac{R(x)^2}{4h_c^2} \right] e^{iKx\cos\beta} \right\} \tag{A14-d}$$

$$F_6 = \rho g K A \gamma \sin\beta\, e^{-i\omega t}\left\{ \int_L dx\, S_A(x)\, x \left[2 + \frac{R(x)^2}{4h_c^2} \right] e^{iKx\cos\beta} \right\} \tag{A14-e}$$

where the real part of all the above expressions is to be taken, and γ and δ are defined by Equations (A6).

APPENDIX B

HYDRODYNAMIC COEFFICIENTS

APPENDIX B

HYDRODYNAMIC COEFFICIENTS

The hydrodynamic coefficients appearing in the equations of motion are the added inertia coefficients, A_{ij}, associated with the acceleration of the body and the damping coefficients, B_{ij}, associated with the velocity. Except for the axial coefficients, A_{11} and B_{11}, other coefficients are obtained from a strip approximation in which sectional quantities are computed and then integrated over the length of the body to provide three-dimensional results.

ADDED INERTIA COEFFICIENTS

The added inertia coefficient or added mass for axial motion, A_{11}, may be estimated by assuming the vehicle to be an equivalent spheroid. Hence, the added mass is given by[8]

$$A_{11} = -\frac{\alpha_0}{2-\alpha_0} m \tag{B1-a}$$

where

$$\alpha_0 = \frac{2(1-e^2)}{e^3}\left(\frac{1}{2}\log\frac{1+e}{1-e} - e\right)$$

and

$$e^2 = 1 - \frac{4R_c^2}{L^2}$$

All other added inertia terms can be obtained from the strip approximations as follows:

---

[8] Lamb, H. Hydrodynamics, 6th ed., Cambridge 1932.

$$A_{22} = \int_L a_{22}(x)\,dx \quad \text{(B1-b)} \qquad A_{55} = \int_L x^2 a_{33}(x)\,dx \quad \text{(B1-e)}$$

$$A_{33} = \int_L a_{33}(x)\,dx \quad \text{(B1-c)} \qquad A_{26} = A_{62} = \int_L x a_{22}(x)\,dx \quad \text{(B1-f)}$$

$$A_{66} = \int_L x^2 a_{22}(x)\,dx \quad \text{(B1-d)} \qquad A_{35} = A_{53} = -\int_L x a_{33}(x)\,dx \quad \text{(B1-g)}$$

where integration is carried over the length of the body and $a_{22}(x)$ and $a_{33}(x)$ are the added masses of a section at location x in the sway and heave modes, respectively. If we assume that the sections are deeply submerged such that any forced motion does not disturb the calm water surface, then the added masses for circular cylinders moving near a rigid wall are given by[7]

$$a_{22}(x) = a_{33}(x) = \rho \pi R(x)^2 \left[1 + \frac{R(x)^2}{2 h_c^2}\right] \quad \text{(B2)}$$

where R(x) is the circular cylinder radius at location x.

DAMPING COEFFICIENTS

When the body is submerged far enough below the water surface such that no disturbance on the calm water surface is generated by forced body motion, the so-called wavemaking damping or potential forces depending linearly on body velocity are zero. There are, however, viscous forces acting on the body which typically depend upon the square of the velocity, and therefore cannot be substituted directly into the linear equations of motion.

We can, however, use the method of equivalent linearization[9] to replace the nonlinear drag by pseudo-linear terms such that the equations of motion may be solved.

The axial viscous drag can be written in terms of the submarine derivative X_{uu} given in Reference 5 as

$$F_D = X_{uu} \left| \dot{\xi}_1 \right| \dot{\xi}_1$$

If we attempt to cast the drag in the form $B_{11} \dot{\xi}_1$, it is clear that the coefficient B_{11} is a time varying function of velocity. The equivalent linearization method[9] replaces $|\dot{\xi}_1|$ by the time averaged quantity, $\frac{8\omega}{3\pi} \left| \xi_{01} \right|$, such that the damping coefficient may be written as

$$B_{11} = \frac{8}{3\pi} X_{uu} \, \omega \left| \xi_{01} \right| \qquad \text{(B3-a)}$$

where $|\xi_{01}|$ is the amplitude of the displacement and the factor, $8/3\pi$, is the coefficient of the first term in the Fourier expansion of $|\dot{\xi}_1| \dot{\xi}_1$. The damping coefficient, B_{11}, is now time independent, although still dependent upon the amplitude of the motion. The coefficient may, however, be substituted into the equation of motion, with an arbitrarily chosen amplitude, and the equation then iterated until a convergent solution for ξ_{01} is obtained.

The other damping coefficients may be derived from simple cross-flow drag considerations and the strip approximation. The cross-flow drag per unit length on a circular section has the form

$$F_D/L = 1/2 \; C_D \, \rho D(x) \left| v_i \right| v_i$$

---

[9] Thomson, W. T., "Mechanical Vibrations," Prentice-Hall, Inc., Englewood Cliffs, N.J., 1963.

where the v_i is the transverse velocity of the section of diameter, $D(x)$, and may be associated with $\dot{\xi}_2$, $\dot{\xi}_3$, $x\dot{\xi}_5$, or $x\dot{\xi}_6$. The symbol, C_D, is the drag coefficient of a circular cylinder. Casting the drag in terms of the coefficients, B_{ij}, replacing $|\dot{\xi}_i|$ by $\frac{8\omega}{3\pi}\left|\xi_{oi}\right|$, and integrating over the length of the body, the damping coefficients, B_{ij}, are expressed as

$$B_{22} = \frac{8}{3\pi}\rho C_D \omega |\xi_{02}| \int_L R(x)\,dx \qquad \text{(B3-b)}$$

$$B_{62} = \frac{8}{3\pi}\rho C_D \omega |\xi_{02}| \int_L x R(x)\,dx \qquad \text{(B3-c)}$$

$$B_{53} = -\frac{8}{3\pi}\rho C_D \omega |\xi_{03}| \int_L x R(x)\,dx \qquad \text{(B3-d)}$$

$$B_{55} = \frac{8}{3\pi}\rho C_D \omega |\xi_{05}| \int_L |x| x^2 R(x)\,dx \qquad \text{(B3-e)}$$

$$B_{33} = \frac{8}{3\pi}\rho C_D \omega |\xi_{03}| \int_L R(x)\,dx \qquad \text{(B3-f)}$$

$$B_{26} = \frac{8}{3\pi}\rho C_D \omega |\xi_{06}| \int_L |x| x R(x)\,dx \qquad \text{(B3-g)}$$

$$B_{35} = -\frac{8}{3\pi}\rho C_D \omega |\xi_{05}| \int_L |x| x R(x)\,dx \qquad \text{(B3-h)}$$

$$B_{66} = \frac{8}{3\pi}\rho C_D \omega |\xi_{06}| \int_L |x| x^2 R(x)\,dx \qquad \text{(B3-i)}$$

APPENDIX C

EQUATIONS FOR DYNAMIC STABILITY OF THE MOORED BODY SCHEME A

APPENDIX C

EQUATIONS FOR DYNAMIC STABILITY OF THE MOORED BODY SCHEME A

In the following section, the criteria for horizontal and vertical plane dynamic stability of the moored body in a steady current are developed from the linearized equations of motion. The equations are formulated relative to a body fixed coordinate system where the origin is located on the body axis above the cable attachment point. The formulation and notations used follow the standard equations for submarine motion given in Reference 5 with the exception that the positive z axis is taken to be upward and the positive y axis to port as shown in Figure 33.

The equations are written for small perturbations from the equilibrium position. It is assumed that at equilibrium the cable is vertical but the body may have an equilibrium pitch and heading angle relative to the current denoted by α_o and β_o, respectively, as shown in Figure 33. The quantities u, v, and w are the perturbation velocities along the body x', y', and z' directions, respectively, and q and r are the perturbation angular velocities in pitch and yaw, respectively. Due to the cable restraint, displacement dependent terms appear in the equations and the perturbation displacements along the body axes are given by $u = \dot{\psi}_1$ $v = \dot{\psi}_2$, $q = \dot{\psi}_5$ and $r = \dot{\psi}_6$. Because the body is vertically restrained by the cable, to first order we must have $\dot{\psi}_3 \approx 0$ and $w \approx U_o \psi_5$ where U_o is the steady current velocity.

VERTICAL PLANE

In the vertical plane the axial and pitch equations are coupled, w and ψ_5 are kinematically related by $w \approx U_o \phi_5$.

Axial Force:

$$m\dot{u} + m z_G \dot{q} = \rho/2 \, L^3 X'_{\dot{u}} \dot{u} - \frac{T_s \cos\alpha_o}{h_B} \psi_1 + \frac{T_s R_o \cos\alpha_o}{h_B} \psi_5 \tag{C1}$$

Pitch Moment:

$$\begin{aligned} I_y \dot{q} + m z_G \dot{u} - m x_G (\dot{w} - U_o q) &= \rho/2 \, L^5 M'_{\dot{q}} \dot{q} \\ &+ \rho/2 \, L^4 M'_{\dot{w}} \dot{w} + \rho/2 \, L^4 M'_q U_o q + \rho/2 \, L^3 M'_w U_o w \\ &- \left[T_s R_o (1 + R_o/h_B) - m g z_G \right] \cos\alpha_o \, \psi_5 + \frac{T_s R_o}{h_B} \cos\alpha_o \, \psi_1 \end{aligned} \tag{C2}$$

With $w = U_o \psi_5$ and $\dot{w} = U_o q$ the above equations may be rewritten, respectively

$$\left[L^3 (X'_{\dot{u}} - m') s^2 - \frac{T_s \cos\alpha_o}{\rho/2 \, h_B} \right] \psi_1 + \left[-L^4 m' z'_G s^2 + \frac{T_s R_o \cos\alpha_o}{\rho/2 \, h_B} \right] \psi_5 = 0 \tag{C3}$$

$$\begin{aligned} &\left[-L^4 m' z'_G s^2 + \frac{T_s R_o \cos\alpha_o}{\rho/2 \, h_B} \right] \psi_1 + \left[L^5 (M'_{\dot{q}} - I'_y) s^2 \right. \\ &\left. + L^4 U_o (M'_{\dot{w}} + M'_q) s + L^3 U_o^2 M'_w - \left\{ \frac{T_s R_o (1 + R_o/h_B) - m g z_G}{\rho/2} \right\} \cos\alpha_o \right] \psi_5 \\ &= 0 \end{aligned} \tag{C4}$$

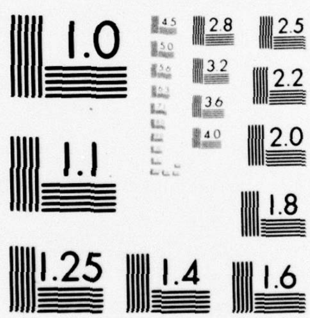

MICROCOPY RESOLUTION TEST CHART

NATIONAL BUREAU OF STANDARDS-1963-A

where $I'_y = \dfrac{I_y}{\rho/2\, L^5}$, $z'_G = \dfrac{z_G}{L}$, $m' = \dfrac{m}{\rho/2\, L^3}$, and $s = \dfrac{d}{dt}$

In a rigorous sense the nature of the solution for coupled axial and pitch motion is determined by the roots of a quartic characteristic equation, and the roots may be obtained in a variety of ways.

The vertical plane stability, however, may be more easily examined by considering a simplified form of Equations (C1) and (C2).. Under the assumption that $z_G = 0$ and the cable length, h_B, is very large with respect to the body radius, R_o, Equations (C1) and (C2) can be decoupled and the characteristic equation for pitch motion ψ_5 reduces to a quadratic of the form

$$as^2 + bs + c = 0 \tag{C5}$$

where

$$a = \rho/2\, L^5 \left(M'_{\dot q} - I'_y\right)$$

$$b = \rho/2\, L^4 U_o \left(M'_{\dot w} + M'_q\right)$$

$$c = \rho/2\, L^3 U_o^2 M'_w - T_s R_o \cos\alpha_o$$

For the case of the Moored Body scheme A, a and b are both negative (See Table IV) therefore the sign of c determines the pitch stability characteristics. Roots with negative real parts are obtained when $c < 0$, which means that

$$\rho/2\, L^3 U_o^2 M'_w \leq T_s R_o \cos\alpha_o . \tag{C6}$$

For M'_w positive, the moored body is stable at low current speeds but unstable at higher current speeds. For M'_w negative; stability is obtained at all current speeds.

In Equation (C4) it may be noted that the restoring moment provided by the vertical center of gravity acts in the same sense as the cable tension when $z_g < 0$ and thus provides an additional stabilizing effect to the pitch motion as expected. Although Equations (C3) and (C4) cannot rigorously be decoupled when $z_G \neq 0$, an approximate condition for vertical plane stability which includes the effect of vertical center of gravity but neglects any surge coupling is,

$$\frac{\rho}{2} L^3 U_o^2 M'_w \leq (T_s K_c - mg z_G) \cos\alpha_o \tag{C7}$$

HORIZONTAL PLANE

The coupled linear equations for lateral and yaw motion of the moored body in a steady current are:

Lateral Force:

$$m(\dot{v} + U_o r + x_G \dot{r}) = \frac{\rho}{2} L^4 Y'_{\dot{r}} \dot{r} + \frac{\rho}{2} L^3 Y'_{\dot{v}} \dot{v}$$

$$+ \frac{\rho}{2} L^3 Y'_r U_o r + \frac{\rho}{2} L^2 Y'_v U_o v - \frac{T_s}{h_8} \psi_2 \tag{C8}$$

Yaw Moment:

$$I_z \dot{r} + m x_G (\dot{v} + U_o r) = \frac{\rho}{2} L^5 N'_{\dot{r}} \dot{r} + \frac{\rho}{2} L^4 N'_{\dot{v}} \dot{v}$$

$$+ \frac{\rho}{2} L^4 N'_r U_o r + \frac{\rho}{2} L^3 N'_v U_o v \tag{C9}$$

The above equations may be rewritten respectively

$$\left[L^3 (Y_{\dot v}' - m') s^2 + L^2 U_o Y_v' s - \frac{T_s}{\rho/2\, h_B} \right] \psi_2$$
$$+ \left[L^4 (Y_{\dot r}' - m' x_G') s + L^3 (Y_r' - m') U_o \right] r = 0 \tag{C10}$$

$$\left[L^4 (N_{\dot v}' - m' x_G') s^2 + L^3 U_o N_v' s \right] \psi_2$$
$$+ \left[L^5 (N_{\dot r}' - I_z') s + L^4 U_o (N_r' - m' x_G') \right] r = 0 \tag{C11}$$

where:

$$m' = \frac{m}{\rho/2\, L^3} \quad , \quad I_z' = I_z / \rho/2\, L^5 \quad , \quad x_G' = \frac{x_G}{L}$$

and s is the Laplace operator, $\frac{d}{dt}$.

Equations (C10) and (C11) form a pair of linear homogeneous differential equations for ψ_2 and r and the roots of the characteristic equation for the above set provide the basic form of the solution.

The characteristic equation is a cubic of the form

$$a s^3 + b s^2 + c s + d = 0 \tag{C12}$$

where:

$$a = \left[(Y_{\dot v}' - m')(N_{\dot r}' - I_z') - (Y_{\dot r}' - m' x_G')(N_{\dot v}' - m' x_G') \right.$$

$$b = \left[Y_v' (N_{\dot r}' - I_z') + (Y_{\dot v}' - m')(N_r' - m' x_G') \right.$$
$$\left. - (Y_r' - m')(N_{\dot v}' - m' x_G') - N_v' (Y_{\dot r}' - m' x_G') \right] \frac{U_o}{L}$$

$$c = \left[Y_v' (N_r' - m' x_G') - N_v' (Y_r' - m') - \frac{T_s (N_{\dot r}' - I_z')}{\rho/2\, L h_B U_o^2} \right] \frac{U_o^2}{L^2}$$

$$d = - \frac{T_s (N_r' - m' x_G')}{\rho/2\, L h_B U_o^2} \frac{U_o^3}{L^3}$$

If all of the roots of Equation (C12) have negative real parts the body is stable in the horizontal plane. For a cubic equation a necessary and sufficient condition that all of the roots have negative real parts is that:

(a) all coefficients have the same sign.

(b) $bc - ad > 0$ (C13)

REFERENCES

1. Milne-Thomson, "Theoretical Hydrodynamics," Fifth Edition, MacMillan Company, 1968.

2. Newman, J.N., P. Plaia, and E.F. Zarnick, "Pitching Motions of a Moored Submerged Mine in Waves," NSRDC Report 2151, March 1966.

3. St. Denis, M., and W.S. Pierson, "On the Motion of Ships in Confused Seas," Trans. SNAME, Volume 61, 1953.

4. Frank, W., and N. Salvesen, "The Frank Close Fit Ship Motion Computer Program," NSRDC Report 3289, June 1970.

5. Gertler, M., and G. Hagen, "Standard Equations of Motion for Submarine Simulation," NSRDC Report 2510, June 1967.

6. Lee, C.M., and J.N. Newman, "The Vertical Mean Force and Moment of Submerged Bodies Under Waves," Journal of Ship Research, Volume 15, Number 3, September 1971.

7. Kennard, F.H., "Irrotational Flow of Frictionless Fluids, Mostly of Invariable Density," NSRDC Report 2299, 1967.

8. Lamb, H., "Hydrodynamics," Sixth Edition, Cambridge, 1932.

9. Thomson, W.T., "Mechanical Vibrations," Prentice-Hall, Inc., Englewood Cliffs, N.J., 1963.

DTNSRDC ISSUES THREE TYPES OF REPORTS

(1) DTNSRDC REPORTS, A FORMAL SERIES PUBLISHING INFORMATION OF PERMANENT TECHNICAL VALUE, DESIGNATED BY A SERIAL REPORT NUMBER.

(2) DEPARTMENTAL REPORTS, A SEMIFORMAL SERIES, RECORDING INFORMATION OF A PRELIMINARY OR TEMPORARY NATURE, OR OF LIMITED INTEREST OR SIGNIFICANCE, CARRYING A DEPARTMENTAL ALPHANUMERIC IDENTIFICATION.

(3) TECHNICAL MEMORANDA, AN INFORMAL SERIES, USUALLY INTERNAL WORKING PAPERS OR DIRECT REPORTS TO SPONSORS, NUMBERED AS TM SERIES REPORTS; NOT FOR GENERAL DISTRIBUTION.